

Lewis River Spawning Gravel Evaluation

Final Year One Report

Prepared for:
PacifiCorp
825 Multnomah
Suite 1500
Portland, OR 97232

Prepared by:
Stillwater Sciences
1314 43rd Street
Seattle, WA 98105

April 2006



Table of Contents

1	INTRODUCTION AND BACKGROUND.....	1
1.1	Tasks (Evaluation Objectives)	1
1.2	Approach.....	1
1.3	Evaluation Area	2
1.4	Fish Resources	3
1.5	Project Schedule.....	5
2	METHODS	6
2.1	Aerial Photography	6
2.2	Facies Mapping.....	6
2.3	Pebble Counts	7
2.4	Spawning Habitat Mapping	8
2.5	Sediment Transport and Spawning Habitat Modeling	8
2.5.1	Tracer gravel	8
2.5.2	EASI modeling.....	9
2.5.3	Application of the ESCAPE model.....	9
3	RESULTS AND DISCUSSION	11
3.1	Chinook Salmon Habitat Limitation	11
3.1.1	Spawning gravel availability and use.....	11
3.1.2	Spawning gravel preferences within the upper reach.....	12
3.1.3	Fall Chinook salmon population dynamics	13
3.2	Channel Morphology	14
3.2.1	Changes in historical channel morphology	14
3.2.2	Spawning gravel dynamics	15
3.3	Conclusion	17
4	MONITORING PLAN	18
4.1	Minimum Discharge	18
4.2	Spawning Habitat Use Monitoring	18
5	GRAVEL AUGMENTATION STRATEGY.....	19
5.1	Spawning Gravel Augmentation Strategy Options	19
5.2	Spawning Gravel Augmentation Monitoring Plan Design and Review	19
6	2006 AND 2007 FIELDWORK.....	21
7	LITERATURE CITED	22

List of Tables

Table 1. Periodicity chart for various life stages of fish species (with known life history information) in the Lewis River basin..... 4
Table 2. Size classes for each particle type used for facies mapping..... 7
Table 3. Input parameter descriptions and base model values for the Superimposition Model, ESCAPE 5. 10
Table 4. Female spawner escapement and redd counts in the upper reach of the Lewis River below Merwin Dam. 12

List of Figures

Figure 1. Location map of the Evaluation Area in southwestern Washington.
Figure 2. Example of tracer gravel grid.
Figure 3. Chinook salmon effective females and effective eggs versus escapement from ESCAPE output.
Figure 4. Spawning habitat maps.
Figure 5. Female spawner escapement and females to redds ratio in the Lewis River from 1984 to 1999.
Figure 6. Female to redds ratio versus female escapement in the Lewis River.
Figure 7. Chinook egg mortality versus female escapement from ESCAPE output.
Figure 8. Comparison of 1938 photos to 2005 photos.
Figure 9. Scarp on static point bar at RM 19.2 on the north bank of the Lewis River.
Figure 10. Static point bar with scarp with riparian vegetation.
Figure 11. Riparian forest at RM 15.2 on south bank of the Lewis River.
Figure 12. Detail of spawning dunes in WDFW spawning index reach 1.

List of Appendices

Appendix A: Background information on Project relicensing.
Appendix B: Section 7.2 from the Lewis River Hydroelectric Projects Settlement Agreement.
Appendix C: Schedule 7.2 from the Lewis River Hydroelectric Projects Settlement Agreement.
Appendix D: EASI sediment transport model.
Appendix E: WDFW escapement and redd count tables.
Appendix F: Facies mapping.

1 INTRODUCTION AND BACKGROUND

As part of the Lewis River relicensing process, PacifiCorp contracted with Stillwater Sciences to (1) develop and implement a salmon spawning gravel evaluation to characterize current conditions, (2) develop a long-term gravel monitoring plan for the Lewis River downstream of Merwin Dam, and (3) to develop a gravel augmentation strategy if results of the study indicate that spawning gravels are limiting salmonid populations (Appendix A). The evaluation area encompasses a roughly 10-mile (6.2 km) reach of the Lewis River, starting from Merwin Dam (RM 19.5) downstream to Eagle Island (RM 9.8). The study is expected to last three years. This particular study was required under the terms of the Lewis River Hydroelectric Project Settlement Agreement, as described in Section 7.2 (Appendix B). This report includes the results of only the first of three years of evaluation. Final results of the three-year study will be reported in a supplement to the Final Report. The results will be used as a benchmark from which to measure future changes in spawning gravel quality and quantity.

1.1 Tasks (Evaluation Objectives)

As described in the Scope of Work (Appendix C), there are four fundamental tasks to be completed in this evaluation:

- (1) Determine the extent of suitable spawning gravel in the Lewis River below Merwin Dam (RM 19.5) to the downstream end of Eagle Island (RM 9.8)
- (2) Develop a spawning gravel monitoring program for measuring future changes in gravel quantity and characteristics, and
- (3) Provide a means for determining when spawning gravel augmentation or retention efforts are warranted, and
- (4) Propose a gravel augmentation strategy that addresses the quality of gravel to be emplaced the timing of the augmentation, and the methods to be used.

A primary concern for the Lewis River is determining if existing areas of spawning habitat are sufficient to accommodate future spawning populations of Chinook and coho salmon and steelhead if current recovery efforts targeted at rebuilding depleted stocks are successful. Gravel supply to reaches downstream of Merwin Dam are limited due to sediment capture by upstream dams, so understanding potential future reductions in spawning habitat is an important goal of the study.

1.2 Approach

The approach used in this evaluation included both field and numerical modeling components. The field component consisted of (1) taking new low-elevation, high-resolution aerial photographs of the study reach, from which base maps were created, and (2) delineating all substrate deposits in the active channel as well as all spawning habitat [used by anadromous salmonids in the 2005 spawning season] onto the new base maps. The latter procedure, termed “facies mapping,” measures grain sizes at gravel bars and other depositional areas in a way that allows one to map the distribution of suitably sized spawning gravels throughout the study reaches. The aerial photos and annotated base maps were geo-referenced and brought into a GIS to allow for subsequent spatial analyses.

These detailed substrate facies maps will be coupled with numerical simulation models to achieve the evaluation objectives described below in Section 1.1. The models serve two purposes. The *Sediment Transport Model* relates the distribution and volume of existing river bed sediments to the sediment

transport capacity of the river, which is a function of discharge during high flow events, sediment supply, and channel geometry. The *Habitat Limitation Model* simulates varying levels of salmonid escapement and coincident use of available spawning gravel, to guide evaluation of potential changes in spawning gravel quality and area. This combination of field results and numerical modeling requires three steps: Step 1 involves delineating the current extent of potential spawning gravel to form a baseline for future monitoring, Step 2 is determining a discharge criteria (i.e. magnitude of flood that results in gravel mobilization) that would trigger monitoring of spawning gravel extent during the license term, and Step 3 is determining whether gravel augmentation needs to be implemented based upon established criteria as a result of the spawning gravel monitoring. Detailed explanation of these steps is provided in Sections 3, 4, and 5 below.

Along with the new data generated from this project, the analysis uses results from previous studies prepared for the relicensing of PacifiCorp's Merwin Dam. These studies include: (WTS) 3 Report: Stream Channel Morphology and Aquatic Habitat Study, WTS 3 Appendix 2: Substrate Samples, WTS 3 Appendix 3: Spawning Gravel Samples, Sediment input budget, Memorandum: Review of Draft Report on Lewis River Geomorphology Study (Stillwater Sciences 2002), as well as spawning ground surveys conducted yearly by the Washington Department of Fish and Wildlife (Shane Hawkins, pers. comm., 28 March 2006).

1.3 Evaluation Area

The Lewis River basin is located on the western slopes of the Cascade Mountain Range. Two volcanic peaks, Mount Adams and the recently active Mount St. Helens, lie on the northern and eastern extremities of the basin. Foothills in the central portion of the watershed are generally steep and forested and extend up to approximately 914 m (3,000) ft mean sea level. Downstream of Lake Merwin, the Lewis River enters a terrain of rolling hills that eventually shift to the essentially flat "Woodland Bottoms" near the river's confluence with the Columbia River. Forested areas are dominated by conifer, including Douglas-fir (*Pseudotsuga menziesii*) and western hemlock (*Tsuga heterophylla*) forest types. Upland deciduous and mixed conifer-deciduous forests also occur in the watershed. The Lewis River basin has the predominantly temperate marine climate typical of the Pacific Northwest. A narrow range of temperatures, dry summers, and mild but rainy winters are typical. Terrain influences the rainfall and temperature patterns, with lower elevations experiencing warmer temperatures and less rainfall and higher elevations receiving more rain, snow, and cooler temperatures. Average annual precipitation near the mouth of the watershed is 94 cm (37 in), while average annual precipitation on Mount Adams exceeds 356 cm (140 in). Snowfall is minimal at lower elevations but greater than 500 cm/yr (200 in/yr) at elevations over 3,000 feet. In the warmest summer months, afternoon temperatures range from the mid 70s °F to the lower 80s °F, with nighttime temperatures in the 50s °F. Maximum temperatures exceed 90 °F on 5 to 15 days each summer. Temperatures in the foothills and higher elevations are slightly lower than those recorded in the valleys.

There are four hydropower projects on the Lewis River, with the Merwin Dam being the lower-most in the system. These four hydropower projects are the dominant feature in the central portion of the Lewis River basin, controlling discharge of both water and sediment. Large reservoirs are formed by Swift, Yale and Merwin dams. Generally the surrounding area is rural and wooded, with forest lands dominating the landscape around Swift Creek Reservoir, transitioning to more mixed forestry and rural uses in the vicinity of Yale Lake and Lake Merwin. The USDA Forest Service (USFS) manages extensive portions of the upper basin, and the Washington Department of Natural Resources (WDNR) manages sizeable holdings in the central basin. PacifiCorp and Cowlitz Public Utility District (PUD) own

and manage lands in the vicinity of the four projects while the lower basin is largely in private ownership. The entire basin is within the jurisdiction of three counties: Cowlitz, Clark, and Skamania.

This spawning gravel evaluation focuses on the portion of the Lewis River downstream of the Merwin Dam (RM 19.5) to just below Eagle Island (RM 9.8). A map of the evaluation area is presented in Figure 1. The upper portion of this reach passes through a highly confined channel from RM 19.5 to approximately RM 15.0, where channel confinement is moderate. The evaluation reach is a low gradient channel with pool-riffle morphology. The downstream extent of this evaluation reach was chosen because (1) the channel widens significantly downstream of Eagle Island, (2) the proportion of sand within the gravel matrix increases at the lower end of Eagle Island, due in part to geology and the tidal backwater effect from the Columbia River, and (3) the majority of salmon spawning in the mainstem Lewis River occurs upstream of RM 9.2.

1.4 Fish Resources

There are four anadromous fish species of concern in the evaluation area: Chinook salmon, coho salmon, steelhead, and chum salmon. A summary of their life history timing is presented in Table 1. Detailed discussions of their habitat and life history requirements are presented in Bio-Analyst et al. 2003, Section 4.1.

Table 1. Periodicity chart for various life stages of fish species (with known life history information) in the Lewis River basin.^{1, 2}

SPECIES	LIFE STAGE	JAN	FEB	MAR	APR	MAY	JUN	JUL	AUG	SEP	OCT	NOV	DEC
Spring Chinook	Adult Migration												
	Spawning												
	Fry Emergence												
	Rearing												
	Juv. Outmigration												
Fall Chinook	Adult Migration												
	Spawning												
	Fry Emergence												
	Rearing												
	Juv. Outmigration												
Coho Salmon	Adult Migration												
	Spawning												
	Fry Emergence												
	Rearing												
	Juv. Outmigration												
Summer Steelhead	Adult Migration												
	Spawning												
	Fry Emergence												
	Rearing												
	Juv. Outmigration												
Winter Steelhead	Adult Migration												
	Spawning												
	Fry Emergence												
	Rearing												
	Juv. Outmigration												
Chum Salmon	Adult Migration												
	Spawning												
	Fry Emergence												
	Rearing												
	Juv. Outmigration												
Sea-run Cutthroat	Adult Migration												
	Spawning												
	Fry Emergence												
	Rearing												
	Juv. Outmigration												
Pacific Lamprey	Adult Migration												
	Spawning												
	Emergence												
	Rearing												
	Juv. Outmigration												
Kokanee (Cougar Cr.)	Adult Migration												
	Spawning												
	Fry Emergence												
	Rearing												
	Juv. Outmigration												
Bull Trout	Adult Migration												
	Spawning												
	Fry Emergence												
	Rearing												
	Juv. Outmigration												

¹ Periodicity is based on peak times and fishes of natural or wild origin.

² This source of this table is Bio-Analyst et al. 2003, Section 4.1.

Of the anadromous fish species present, Chinook salmon are the most abundant. There are two distinct runs of Chinook salmon in the Lewis River: the less abundant spring run, and the more abundant fall run. Although coho salmon and steelhead spawn in the mainstem channel, it does not offer ideal spawning habitat for these species given their typical preferences. This spawning gravel evaluation focuses on both spring- and fall-run Chinook salmon because they are the dominant species spawning in the mainstem downstream of Merwin Dam. Their spawning activity is the main driver of the ample physical evidence for spawning. While the spawning activity of coho salmon and steelhead is observable, their efforts are overwhelmed by the preponderance of spawning Chinook salmon. Furthermore, impacts to spawning

habitat in the Lewis River below Merwin Dam will have the greatest impact on Chinook salmon as compared to the other species. In general, many of the results presented in this spawning gravel evaluation are applicable to coho salmon and steelhead, and will be discussed where appropriate. There is little evidence for spawning of chum salmon in the evaluation area; therefore, they have been left out of the discussion.

1.5 Project Schedule

This project began in June 2005, in coordination with PacifiCorp and the Aquatic Coordination Committee (ACC), a group of federal, state, tribal and stakeholder interest representatives. Field mapping of potential spawning habitat took place in late September 2005, after aerial photography was completed in August 2005. A draft Evaluation Report summarizing Year 1 monitoring effort was completed and submitted to the ACC in December 2005. Subsequent reports will follow monitoring efforts over the next 2 years. Final Year 2 and Year 3 Evaluation Report will be completed in early 2007 and 2008, respectively.

2 METHODS

The methods section is divided into the following four major topic areas:

- aerial photography of evaluation reach,
- bed surface textural analysis,
- spawning habitat utilization, and
- sediment transport modeling.

2.1 Aerial Photography

High-resolution (1:500 scale, ~914 m [3,000 ft] above the mean terrain elevation) aerial photographs were taken of the evaluation area from Merwin Dam (RM 19.5) to Eagle Island (RM 9.8) on 8 August 2005 by David Smith & Associates Inc. of Portland, Oregon. The average daily flow at the USGS Lewis River at Aerial gage (# 14220500) during the time the photographs were taken was 2,059 cfs. Ground control points (GCP) surveyed in 1996 by Minister & Glaeser of Vancouver, Washington were used to georeference and orthorectify the photographs after they were transferred to a digital format. The pixel resolution of the digital images is 0.15 m/pixel (0.5 ft/pixel). The images cover a narrower field of view than the photographs (approximately 300 m [1,000 ft] of floodplain on each bank) because of the limited number of GCP along the Lewis River in the evaluation area. The digital aerial images made from the photogrammetry and control points were designed to conform to National Map Accuracy Standards (NMAS) for a 1 cm = 1,667 m (1 in = 200 ft) horizontal and 1.5 m (5-ft) contour vertical accuracy. These digital aerial photographs were used as the base map for field mapping.

2.2 Facies Mapping

Facies mapping was used within the field evaluation because it allows for relatively rapid, robust, and repeatable classification of the stream bed surface composition. Within this project, facies mapping serves two purposes: 1) it provides a map of river bed particle size distribution throughout the evaluation reach, and 2) it clearly delineates the distribution and area of spawning-sized gravel (i.e., potential available spawning habitat) throughout the evaluation reach in the season of mapping. In facies mapping, the primary descriptor used is the dominant particle size class on the bed surface, modified by one or two subordinate particle size classes (Buffington and Montgomery 1999). The method is hierarchical: in *Level I*, the surface is classified according to the proportional occurrence of the three most prevalent grain classes (i.e., silt, sand, gravel, cobble, and boulder) in ascending order; in *Level II*, the most frequent grain size is sub-divided according to a classification based on phi-size class. For example, *scG* is referred to as sandy-cobbly gravel. The qualifying criteria for inclusion are that an individual grain size comprises $\geq 5\%$ of the surface area, or that the two sub-ordinate classes together comprise $\geq 10\%$. Where the qualifying criteria are not met, the surface may be classified according to the one or two most frequent grain classes (e.g., *C* or *gC*). Using a ternary diagram, this gives 15 possible combinations for any three grain sizes. The *Level II* classification is done in the same manner as the *Level I* (i.e., arranging the 3 most frequent phi-size classes in ascending order to give 15 possible combinations). *Level II* classifications include gravel (very fine [*vf*], fine [*f*], medium [*m*], coarse [*c*], very coarse [*vc*]) cobble (*f*, *c*) and boulders (*f*, *m*, *c*, *vc*). Therefore, combining both classifications, sandy-cobbly gravel is comprised primarily of coarse and very coarse gravel sizes is labeled *scG_{cvc}*. Particle sizes for each of the facies particle type is presented in Table 2.

Table 2. Size classes for each particle type used for facies mapping.

Name	Size class (mm)
Boulder	
very coarse	2048-4096
coarse	1024-2048
medium	512-1024
fine	256-512
Cobble	
coarse	128-256
fine	64-128
Gravel	
very coarse	32-64
coarse	16-32
medium	8-16
fine	4-8
very fine	2-4
Sand	0.0625-2
Silt	0.0039-0.0625
Clay	<0.0039

The initial facies mapping of the evaluation reach took place September 10–19, 2005, from just below Merwin Dam to approximately midway down Eagle Island. Areas were delineated in the field on base maps created from aerial photographs printed on waterproof paper. Observations of the stream bed and mapping were done from a boat while floating down the river. Care was taken when identifying and delineating the boundaries between facies. Sketching of contacts was done as precisely as feasible following procedures similar to standard geologic mapping methods. In some cases it was necessary to extrapolate contacts, such as in the case where a boundary crossed the thalweg through deep water. Each distinct facies was enclosed by a polygon sketched and labeled directly onto field maps. Confirmation and calibration of facies designations were accomplished via frequent pebble counts (see Section 2.3 for detailed explanation).

Once facies mapping was complete, facies designations were double checked against the pebble count data and all map symbols and notation was assessed and unified. Subsequent to the map checks, the field maps were scanned, and all facies contact lines and other data were digitized in a geographic information system (GIS).

2.3 Pebble Counts

Pebble counts were conducted at selected locations within the evaluation reach, using the methods described by Wolman (1954). These were done to corroborate the facies designations made using the rapid field techniques described above. The pebble counts included measuring the intermediate (b) axis for 100 pebbles within each of the sedimentary facies identified along the evaluation reach. To insure that pebble count data accurately represented facies information, approximately three pebble counts were performed for each of the sedimentary facies identified. The location of each pebble count was recorded by a hand-held GPS unit and was also sketched onto the field map. Particle size distribution data from the pebble counts was compared to the facies mapping data and corroboration and modification of facies mapping designations are applied as needed.

2.4 Spawning Habitat Mapping

Spawning habitat extent was mapped onto the base maps from direct observation of spawning activity as well as physical evidence of spawning activity from the prior spawning season. These areas link the particle size information and its response to channel forming flows with the need to determine when gravel augmentation would need to occur. Similar to facies mapping in approach, spawner use of available spawning habitat was mapped onto the field maps from a boat while floating the river. The boundaries of active spawning habitat were sketched onto the field maps based on two indicators that the gravel patch was being used for spawning on a more or less annual basis. The primary indicator of spawner use of gravel patches were new redds or the observation of redd construction. The secondary indicator was the presence of distinctive dunes on the stream bed which are the product of repeat spawning of primarily Chinook salmon, but also by other species. Depth and velocity criteria were not used to delineate boundaries of spawning habitat. The focus area of the spawning habitat mapping was primarily between Merwin Dam and the Lewis River Hatchery (the hatchery) (RM 15.7), although additional spawning habitat was mapped below the hatchery when there was strong evidence to indicate it was present. The sketch maps of spawning habitat were digitized using the same approach as for facies mapping.

2.5 Sediment Transport and Spawning Habitat Modeling

To estimate average annual sediment transport, generate a bedload transport rating curve, and define a critical minimum flow to trigger spawning gravel monitoring, Stillwater Sciences employed direct observations of bed stability coupled with the use of a sediment transport model based on the work of Parker (1990). Model assumptions and limitations are explicitly stated. Several techniques are used to generate empirical data to support application of the models, as described below.

2.5.1 Tracer gravel

The amount of bed material transported downstream of the Project can be used to assess how quickly bed material is leaving the reach. The faster the bed material is leaving the reach, the greater the effect of reduced sediment supply on channel form and aquatic habitat. In general, bedload transport occurs in a gravel bedded river only during a few high flow events, while very little or no bedload transport occurs in the majority of the flow conditions (e.g., Leopold et al. 1964). This evaluation will assess how often sediment is transported under current hydrologic and bedload conditions and how the Project has affected the frequency and magnitude of flow events of sufficient magnitude to initiate sediment transport. In this case tracer gravel is being used as an empirical check on the modeling approach that will be used to predict bedload transport occurred during a certain magnitude of flow. A photograph of a tracer gravel array is presented in Figure 2.

Placing tracer gravel on the bed surface is a method used to identify whether a certain stream discharge (and therefore the shear stress) exceeds that for incipient motion of the stream bed. Incipient motion is a phrase that describes initial movement and transport of the surface particles on the stream bed. Transport is described as volumetric movement, usually en masse, of the particles that compose the streambed material. Over time bedload transport, as a function of discharge frequency, magnitude and duration, is the primary geomorphic agent in rivers that forms the bed morphology of the channel (i.e., spawning habitat) and conveys sediment from the upper watershed downstream. Changes in the balance of energy and mass in a given system have variable outcomes depending on which components vary in combination with other inherent qualities of the system. Natural or anthropogenic alteration of the supply or pattern of sediment, water, or both is often the agents of geomorphic change in a river (Ligon et al. 1995).

2.5.2 EASI modeling

The Enhanced Acronym Series with Interface (EASI) is a bedload transport model for gravel bedded rivers adapted from the Acronym Series of Gary Parker, which incorporates the surface-based bedload equation of Parker (1990). The model employs limited information such as grain size distribution, channel slope, channel cross section, and historical discharge records in order to generate a bedload transport rating curve and a long-term average bedload transport capacity. The output of EASI will help to define a discharge at which monitoring of potential spawning gravel would need to occur in the future. It can also provide a better-than-order-of-magnitude estimate of the long-term average bedload transport rate that can be used for guidance of defining a gravel augmentation intensity. A more detailed description of the model and its assumptions is provided in Appendix D.

The model was run for three scenarios based on reach average data. The first run consisted of reach average data for the reach of the Lewis River above the hatchery (RM 15.7 to RM 19.5). The second run was for reach average data for the reach below the hatchery (RM 9.6 to RM 15.7). Finally a run was done for the entire evaluation area (RM 9.6 to RM 19.5).

The daily average discharge at the USGS Lewis River at Aerial gage (# 14220500) for the period of record 1932 through 2004 was used to generate a flow duration curve that serves as input to EASI model. Reach average surface particle size distribution was generated using the 2005 pebble count data. Three reach average surface particle size distributions were generated: one using the 19 pebble counts upstream of the hatchery, one using the 11 pebble counts downstream of the hatchery, and one using all the 31 pebble counts for the entire evaluation area. Reach average width based on 10 bankfull width measurements from the aerial photos were calculated above and below the hatchery. Average width for the entire reach was calculated based on all the 20 width measurements from the aerial photos. The friction slope used in EASI was based on the reach average value of 0.06% reported in Bio-Analyst et al. 2003, Section 2.3. The model was run for three scenarios based on reach average data.

2.5.3 Application of the ESCAPE model

The ESCAPE model is a spatially explicit model of salmon spawning dynamics that estimates egg mortality caused by redd superimposition. The ESCAPE model considers that limitations on spawning gravels for salmonids often result in superimposition of redds, whereby later arriving female salmonids dig redds on top of existing redds, which causes substantial mortality of eggs deposited earlier (Hayes 1987, McNeil 1964). This has been found to be an important factor limiting Chinook salmon populations in streams where dams capture sediments and reduce supply of gravel to downstream reaches (TID/MID 1992). Spawning gravel availability can greatly influence density-dependent mortality of eggs and fry (e.g., Lestelle et al. 1996).

Using information on adult escapement, observed preference of fish for particular reaches, available spawning gravel area, and redd construction behavior and phenology, the model estimates the number of viable eggs in a given river system at the end of the spawning season. Because the number of eggs predicted by the model is directly related to the number of spawners, it can be used to develop a stock-production relationship. The redd superimposition model was developed to evaluate the effects of Chinook salmon redd superimposition; however, it is suitable for use with other salmonids for which sufficient life history information is available. The ESCAPE model is used to estimate the escapement at which spawning habitat (i.e., spawning gravel area) may be limiting to salmonid populations and the potential consequences of reduced spawning habitat area.

The ESCAPE model requires both spatial (e.g., gravel availability, redd size) and temporal (e.g., length of spawning season, redd defense time) information to accurately describe Chinook salmon migration and

spawning characteristics. Spawning behavior and redd characteristics of Pacific salmon are relatively well understood and make this modeling effort possible. The model output reports "effective" egg production associated with a given escapement—that is, the total number of eggs avoiding superimposition. A similar variable, termed effective females, can also be calculated by dividing the effective egg production by average fecundity.

The variables that we used to parameterize the model are data from the Lewis River when available; otherwise the data are taken from published literature on salmonid life history and habitat requirements and are presented in Table 3. In the model runs for the Lewis River, we use average redd counts from 1971 through 1999 to account for spawner preference for the four index reaches in the upper reach. These preference assignments are assumptions subject to an important caveat. The total number of redds counted does usually reflect the number of females, particularly in situations with limited available spawning habitat; thus the number of redds counted is almost certainly an underestimate of the total female spawners. Therefore, we can assume that the true preference of females in the upper reach is somewhat different than that which we used. Furthermore, if the number of redds usually represents an underestimate of the total females using a given spawning area, then the model is an overestimate of the number of effective females in a given spawning area.

Table 3. Input parameter descriptions and base model values for the Superimposition Model, ESCAPE 5.

Parameter	Description (units)	Base model value
Spatial parameters		
Defended region	Dimensions of defended area (cells, ft ²)	4 x 4, 200
Disturbed region	Dimensions disturbed area (cells, ft ²)	2 x 2, 50
Egg region	Dimensions of egg pocket (cells, ft ²)	2 x 2, 50
X units per cell	Cell width (ft)	3.53
Y units per cell	Cell length (ft)	3.53
Spawner preference	Spawner preference by reach (% of total spawners in reach) by reach number (1, 2, 3, 4)	80, 15, 3, 2
Temporal parameters		
Defense time	Redd defense period (days)	11
Spawning time	Length of spawning run (days)	91
Development time	Length of egg development (days)	135
Other parameters		
Eggs per female	Average fecundity (eggs/female)	4,000
Fraction female	% of escapement composed of spawning females	54

3 RESULTS AND DISCUSSION

Key findings include:

- spawning habitat is likely limiting the local Chinook salmon population,
- available spawning gravel does not appear to be diminished in the upper reach, and
- spawning gravel appears to be stable.

3.1 Chinook Salmon Habitat Limitation

Evaluation of fall Chinook salmon spawning in the Lewis River indicate that the population is likely currently near or at its maximum size due to egg mortality from redd superimposition. Figure 3 shows the relationship between numbers of female salmon and the ESCAPE model predictions of number of effective females or eggs. The key factors determining this relationship are the amount of gravel and the preference of female spawners for upper reaches. We concentrated our assessment of spawning habitat in the upper reach (RM 15–RM 19.5) because this is where the majority of spawning occurs. Much of the information in this section (% females in the escapement, % of spawners spawning in the lower reach) was contributed by Shane Hawkins (Wildlife Biologist, WDFW, Vancouver, Washington, pers. comm., 28 March 2006).

The largest escapement on record occurred in 1989 and was 22,987 fish (this number includes hatchery strays) (Hawkins 1999). An average of 54% of returning spawners are females, thus the maximum number of females that has returned to the river for the period of record is approximately 11,789.

An estimated 7% of total returning spawners spawn in the lower reach. The relatively fewer numbers of fish in the lower reach is due to habitat use differences combined with disparity in the population sizes of the different runs of Chinook salmon in the Lewis River. There are two main runs of Chinook salmon in the Lewis River: the early-spawning stream-type (e.g., spring Chinook salmon) and the late-spawning ocean-type (e.g., fall Chinook salmon). There is a small component of the fall run that are colloquially called “late-brights,” which move into the river in December and January after the November peak of the fall run (S. Hawkins, pers. comm., 28 March 2006). The spring and fall Chinook salmon appear to primarily use the upper reach while the late-brights appear to use the lower reach. The late-brights are possibly strays from other systems (S. Hawkins, pers. comm., 28 March 2006). Because fall Chinook salmon are so abundant compared to the late-brights and spring Chinook salmon, they are the run most likely to be affected by any spawning habitat limitations.

3.1.1 Spawning gravel availability and use

Spawning habitat was mapped based on field evidence of spawning activity including spawning dunes and other signs of previous spawning, as well as spawning activity present during the field work. Spawning habitat maps are presented in Figures 4a–e. In general, very little habitat was mapped in the lower reach (Figures 4a–e), primarily because our methodology was more appropriate for the upper reach where spawning is heavier (i.e., in the lower reach, suitable gravel may not be used because of lack of spawning and thus would not be mapped as suitable). Our mapping yields an extent of spawning habitat utilization in the upper reach of 156,253 m² (1,681,891 ft²). Spawning dunes effectively reduce available spawning habitat by approximately 50% because spawning females tend spawn only on the upstream face and top of the dunes, while avoiding the lee and trough. In the upper reach, 27% (41,630 m² [448,106 ft²]) of the total mapped spawning habitat is comprised of spawning dunes; therefore, 120,815 m² (224,051 ft²) of habitat is unavailable, which brings the total extent of available spawning habitat to

135,438 m² (1,457,840 ft²) in the upper reach. The amount of gravel in the lower reach is 11,838 m² (127,428 ft²), but this is almost certainly an underestimate. The 112,407 m² (1,209,934 ft²) of gravel mapped in 2001 using local experience and professional judgment is a better estimate for the lower reach (Bio-Analyst et al. 2003, Section 2.3).

3.1.2 Spawning gravel preferences within the upper reach

Dams often impede access to historical spawning areas, which may limit population size, especially in areas where spawning habitat downstream of the dam is low in quality or quantity. In many streams with dams, adult salmon seem to overwhelmingly prefer spawning in areas just downstream of the dam (Rogers 1973, Sommer et al. 2001), even when apparently higher quality spawning habitat exists further downstream, which can result in redd superimposition and density-dependent egg mortality. In the Lewis River, some potential spawners are returned to the lower river where they spawn in the vicinity of the hatchery (S. Hawkins, pers. comm., 28 March 2006); however, most fish are left to spawn where they choose, which is primarily in the upper reach below the dam.

An important component of modeling density-dependant habitat limitation is assigning spawner preference for specific spawning patches or index reaches. The best data to use in assigning spawner preference is reach-specific spawner escapement estimates combined with total spawning habitat in each reach. Escapement data for the Lewis River is not index reach-specific, but rather reports escapement estimates for the entire river. However, there are redd count data for four index reaches (Table 4) in the upper reach that can be used to indicate preference trends.

Table 4. Female spawner escapement and redd counts in the upper reach of the Lewis River below Merwin Dam.

Year	Escapement	Number of females	Number of females in upper reach ¹	Index reach ²				Total redds	Females/redds
				1	2	3	4		
1984	7,794	4,209	3,914	473	330	213	91	1,107	3.5
1985	8,323	4,494	4,180	274	215	127	59	675	6.2
1986	12,878	6,954	6,467	252	225	169	79	725	8.9
1987	16,345	8,826	8,208	309	254	177	99	839	9.8
1988	13,766	7,434	6,913	156	182	248	178	764	9.0
1989	21,832	11,789	10,964	334	171	304	148	957	11.5
1990	16,814	9,080	8,444	498	394	360	183	1435	5.9
1991	9,350	5,049	4,696	412	190	135	25	762	6.2
1992	7,153	3,863	3,592	335	201	152	58	746	4.8
1993	7,061	3,813	3,546	178	144	119	58	499	7.1
1994	10,391	5,611	5,218	280	189	217	75	761	6.9
1995	12,274	6,628	6,164	493	283	298	119	1,193	5.2
1996	12,934	6,984	6,495	288	620	393	205	1,506	4.3
1997	8,227	4,443	4,132	237	295	376	104	1,012	4.1
1998	5,123	2,766	2,573	231	297	192	100	820	3.1
1999	2,595	1,401	1,303	104	104	85	0	293	4.45
Average	10,804	5,834	5,426	303	256	223	99	881	6.3

¹ Number of females in upper reach is based upon 7% estimate of spawners spawning in the lower reach (S. Hawkins, pers. comm., 28 March 2006).

² Index reach 1 is from the Lewis River Hatchery (RM 15.7) upstream to RM 16.7, index reach 2 is from RM 16.7 upstream to RM 17.8, index reach 3 is from RM 17.8 upstream to RM 18.5, and index reach 4 is from RM 18.5 upstream to Merwin Dam (RM 19.5) (S. Hawkins, pers. comm., 28 March 2006).

Redd data are less well suited for assigning preference than escapement estimates, particularly where redd superimposition may be occurring. If redd superimposition is occurring, redd counts may underestimate the total number of redds actually constructed because of the difficulty inherent in identifying redds that have been superimposed. Redd counts are useful for monitoring general annual spawner distribution and density in the Lewis River (Table 4). The range of the ratio of females to redds is 3.1 to 11.5 with a mean of 6.3 (Table 4). A plot of the ratio of females to redds against female escapement (Figure 5) shows that as escapement rises, the ratio of females to redds rises, which would be expected if there is limited habitat and strong preference for spawning in particular reaches. Even if the mean number of redds is doubled from 881 to 1,762, the resulting ratio of females to redds is 3:1, which still suggests that redd superimposition is likely occurring in the upper reach.

We used the plot of females to redds ratio versus female escapement (Figure 6a) to iteratively allocate spawner preference to the index reaches for our habitat limitation modeling (Section 3.1.3). By varying the preference allocations that we used in the model runs, we were able to generate a curve based on the output of the escape model that approximates the data from the Lewis River (Figure 6b) as a check on the preference allocations that we made. The final allocations of spawner preference that we made to each index reach is as follows: 80% of females spawned in Index Reach 1, 15% of females spawned in Index Reach 2, 3% of females spawned in Index Reach 3, and 2% of females spawned in Index Reach 4. Section 3.1.2 discusses the results of the escape modeling exercise.

3.1.3 Fall Chinook salmon population dynamics

The number of effective females describes the net output of placed eggs accounting for disturbance by superimposition (see Section 2.3.3). If space available for spawning was unlimited, then the number of effective females would be equal to the number of females in the estimated escapement figures, assuming all females spawned.

There is considerable evidence that redd superimposition resulting in egg mortality is the primary source of density-dependent mortality in the Lewis River fall Chinook salmon population. The female-to-redd ratios shown in Figures 5 and 6a range from 3:1 to 11:1. The ratio should be approximately 1:1 in a population where redd superimposition is not prevalent on the spawning grounds. Even if numbers of redds were significantly underestimated or numbers of females significantly overestimated, it would not explain the very large female-to-redd ratios. The fact that the ratios increase with increasing escapement size is another clear indication that redd superimposition increases at higher escapements. The presence of spawning dunes in the upper reach suggests very heavy spawning use and redd superimposition. The ESCAPE model indicates very high egg mortality even at average escapements (Figure 7). Because the ESCAPE model generates female-to-redd ratios somewhat less than what was observed during spawning surveys, the model may be underestimating egg mortality. Regardless, egg mortality of this magnitude would be exerting a strong density-dependent control on population size. Annual population fluctuations suggest that density-independent mortality factors may also be affecting population size (e.g., during smolt outmigration or ocean rearing). A full time-series analysis using a state-space model would help explain the population dynamics and identify the sources of density-independent mortality that may be resulting in low escapements in some years. The management assumption is that increasing spawning habitat in the upper reaches or increasing the use of the underutilized lower reaches would increase population size. A time-series analysis would be necessary to determine what magnitude of increases in population size could be expected.

3.2 Channel Morphology

Despite bed coarsening, entrenchment, and static channel conditions within the upper reach, there is evidence that there has been rather minimal loss of available spawning habitat and losses are not continuing. The reason is related to previously existing conditions of bulk volume and particle size distribution of the riverbed juxtaposed with the new hydrologic regime imposed by dam operations. The end result is a pattern of bed coarsening and channel entrenchment that remains within the useable size preference by spawning Chinook salmon. The fact that the bed has coarsened in response to interrupted sediment supply is itself a factor in the present apparent stability of spawning gravels in the Lewis River. The upper reach is confined to a bedrock canyon that allows little space for the river to meander, and is a relatively high energy system in comparison with the lower reach. As such, there is an inherently lower gravel extent in the upper reach than the lower due the fundamental differences between process regimes and the geomorphic setting of the two reaches.

3.2.1 Changes in historical channel morphology

In December 1933, a flood that peaked at approximately 129,000 cfs occurred—the highest discharge on record at the USGS Lewis River at Ariel gage (#14220500). This flood likely had a profound impact on channel morphology and spawning habitat in the Lewis River below Merwin Dam, which had been in place for less than two years at the time. The channel condition today is the combined legacy of the effect of Merwin Dam on sediment supply, the 1933 flood, and the hydrologic regime since 1933. In 1938 or 1939, the Army Corps of Engineers took aerial photographs of the evaluation area; the photographs capture the channel condition subsequent to the flood of 1933 and can be used to a benchmark to track changes in the channel since the flood.

The most notable impacts of the flood were probably sediment mobilization and reorganization and resurfacing of point bars throughout the evaluation area, which would also have had removed most riparian vegetation. The 1938 aerial photographs show active point bars, mid-channel bars, and islands with little or no established vegetation, which contrasts sharply with current conditions at the same locations where vegetation is pervasive. This vegetation is evident at the point bar on river left at RM 18.7, the mid-channel bars/islands at RM 14.7, the point bar on river right at RM 13.3, and banks and bars along the south channel of Eagle Island (Figures 8a–g).

In addition to mobilizing point bars, the flood resulted in channel avulsions or meander bend cutoffs in several locations in the lower portion of the evaluation area where the river overtopped its banks. Avulsion is when the channel jumps its bed and takes a new course shortening channel, and is usually the result of high discharge and/or incision. In the 1938 aerial photographs, an avulsion can be seen at the location of the present day Lewis River golf course. The south channel of the Lewis River around Eagle Island appears to be at least a subsidiary channel, if not an avulsion. Furthermore, the south channel was congested with sediment in 1938, and the wetted channel was clearly subsidiary to the main stem, which was formed by the north channel. The contemporary Lewis River at this location flows primarily through the south channel, while the north channel appears to be in the process of being cut off.

In contrast to the lower reach, the upper reach is a confined channel that is relatively straight and probably higher gradient (channel slopes will be surveyed in detail during 2006). The steeper slope and confinement result in sediment transport rates being higher in the upper reach than the lower reach. High sediment transport capacity, combined with proximity to a sediment barrier (Merwin Dam) creates a condition in which sediment is being exported from the reach without replacement (see Section 3.2.2). The bed surface of the upper reach is therefore likely a coarse lag deposit left behind by the 1933 flood, particularly the 0.8-km (0.5 mi) reach immediately below Merwin Dam.

The presence of scarps (Figures 9 and 10 along relict active point bars that are now static indicates that the river is winnowing relatively fine sediment and leaving behind a coarse lag deposit. In an unregulated river, active transport of a readily available sediment supply results in active point bars that scour and fill on a semi-seasonal basis and typically shoal smoothly into the thalweg or deepest portion of the channel. The presence of riparian vegetation on formerly active point bars and floodplains indicates pervasive channel encroachment (Figures 10 and 11). In an unregulated channel, active bedload transport and relatively frequent flooding minimize riparian vegetation in regularly inundated areas of the river. Vegetation encroachment is a feature common to many regulated rivers due to interrupted sediment supply and attenuation of high flows.

The lower reach has probably not changed much since the dam was constructed, apart from an increase in riparian vegetation. This is due in part to sediment supplied to the reach from Cedar Creek as well as the upper reach. Overall, the bed surface of the lower reach is finer and more mobile than in the upper reach. There is ample evidence that the bed load is mobile, such as active point bars, deposits of alluvium surrounding the trunks of riparian trees on the left bank at RM 14.5 (probably as result of the 1996 flood), and actively migrating multi-thread channels and mid-channel bars just upstream of Eagle Island.

Most of the bars and bed features visible in the 1938 aerial photographs are likely still present in the upper reach because no flood of the magnitude of the 1933 flood has occurred in the intervening years (see sediment transport discussion in Section 3.2.2 preliminary EASI modeling results). The flood of 1996 was the second largest flood on record, and had a minimal effect on overall bed condition. Spawning dunes in the upper reach were planed off, and some rearrangement of spawning areas occurred (S. Hawkins, pers. comm., November 2005; F. Shrier, pers. comm., April 2005). The minimal effects reported by professional with a long history on the river corroborate the proposition that the present condition of the bed of the Lewis River is the result of the 1933 flood.

3.2.2 Spawning gravel dynamics

Despite the changes in channel morphology discussed above, it does not appear that spawning gravel quantity has changed since the dam was built (at least since the 1933 flood), and is not likely to change in the near future. The evidence for this includes (1) spawning habitat near the dam that has not changed since 1933, (2) sediment transport modeling results showing relatively low average annual sediment transport, (3) tracer experiments showing that discharge as great as 3.5-year recurrence interval transports little sediment, and (4) the presence of spawning dunes. Each of these is discussed in detail below.

3.2.2.1 Historical spawning analysis

The spawning gravel patches immediately below the dam are those at greatest risk of change because the effects of lack of replacement gravels from upstream typically would be most evident just downstream of the dam. There are still suitable spawning gravels just downstream of Merwin Dam, however, including a spawning riffle 0.40 km (0.25 mi) downstream with a D_{50} of 50—well within the suitable range for Chinook salmon and heavily used by these fish under current conditions. The 1933 flood does not appear to have coarsened this riffle to the point where it is unusable by spawning salmon. The riffle does not appear to have significantly changed since the 1938 photos were taken; however, the spawning riffle may have been reduced in size by the flood, with little change since. The fact that this riffle is usable and hasn't changed since at least 1938 strongly suggests that spawning gravels are not being transported even at the highest flows.

3.2.2.2 Preliminary EASI model results

EASI modeling was performed for both the upper and lower reaches in the evaluation area, using appropriate input parameters for each. The results should be viewed as preliminary because the accuracy of certain parameters was based on relatively coarse estimates. For example, a reach-average slope of 0.0006 was used, which was based on USGS topographic maps (Bio-Analyst et al. 2003, Section 2.3) rather than measured in the field. The reach-average sediment transport rates used in the model (derived from particle-size distribution and hydrologic data for the 74 years since Merwin Dam was constructed) were 90 tons/year in the upper reach and 360 tons/year in the lower reach. It should be noted that the general accuracy of sediment transport rate calculations is a factor of two to three (i.e., if the calculated rate is 1, the actual rate normally falls between 0.3 to 3, and most likely between 0.5 to 2), and thus, the transport rate for the upper and lower reaches should be interpreted as a range of from 45 to 180 tons per year, and 180 and 720 tons per year, respectively. These transport rates express reach-average transport rates averaged over the past 74 years, and not sediment transport rates for any one year. In most years sediment transport rates will be much lower. Only during geomorphically significant high flows, such as the 1996 flood, will any appreciable volume of sediment be transported. The difference in the transport rates is primarily a function of the particle size difference in each of the reaches; the bed of the lower reach is finer overall and thus more easily mobilized.

To put the reach-average transport rates into perspective, the 90 tons/year and 360 tons/year bedload transport rates translate to a long-term average of approximately 0.0030 to 0.0122 cm/yr (0.0012 to 0.0048 in/year) of bed degradation, or approximately 0.03 to 0.89 cm (0.01 to 0.35 in) of lost gravel in the 15.7-km (9.8-mi)-long and 99-m (325-ft)-wide reach over the 74 years. It needs to be noted, however, that degradation resulting from reduced bedload supply starts from the upstream end of the reach and propagates downstream, and thus, channel degradation should be most evident at the upstream end. In addition to gravel loss, there should also be bed coarsening associated with the decreased bedload supply and bed incision. The coarser surface sediment in the upper reach is probably at least partly due to channel incision over the past 74 years.

A key parameter predicted by the EASI model is the discharge at which potentially observable sediment transport occurs. This is done in EASI by calculating Shield's stresses at different flows and developing a Shield's stress rating curve (see Appendix D for details). The Shield's stress is then compared with a reference Shield's stress, which is defined as the Shield's stress at which dimensionless bedload transport equals a very small value of 0.00218 (see Parker 1990 for details). The reference Shield's stress is very close to critical Shield's stress, and thus, the bed can be considered to be at incipient motion when the calculated Shield's stress is equal to the reference Shield's stress. In this preliminary modeling exercise, incipient motion is predicted to occur at a discharge of approximately 56,000 cfs in the upper reach and 42,000 cfs in the lower reach, which correspond to 7.7-year and 3.7-year recurrence interval flows, respectively, based on peak flow records from 1932 to 2005. Incipient motion generally occurs at approximately 2- to 3-year recurrence interval flows in gravel-bedded streams (Leopold et al. 1964). Considering potential coarsening over the past 74 years due to the interrupted bedload supply, an increase of incipient motion flow to a level of the 7.7-year recurrence interval flow at the upstream and 3.7-year recurrence interval flow at the downstream reach is reasonable.

3.2.2.3 Tracer gravel

As a quantitative test of the EASI model predictions of bed particle size movement, tracer particles were placed at three sites in the upper reach (Figures 4a–e). Between 1 October 2005 and 5 February 2006, the maximum 1-day average flow at the USGS Lewis River at Ariel gage (# 14220500) was 28,952 cfs (on 12 January 2006). On 15 March 2006, flows had dropped low enough (approximately 1,800 cfs) to allow a site visit to view the tracer rocks. At the first site, the array of tracer rocks had not moved—the rocks

were covered with periphyton and showed no signs of scour. This result is consistent with the EASI model prediction that no sediment transport will occur at that site until discharge exceeds about 56,000 cfs. At Site 2, the site with the smallest particle size distribution, the 3 m x 3 m (10 ft x 10 ft) array of painted rocks had expanded into an approximately 9.1 m x 9.1m (30 ft x 30 ft) area, indicating that some rocks had begun to move but not the entire bed. The discharge at which the EASI had predicted incipient motion would occur at this site was 42,000 cfs, somewhat lower than the actual maximum daily average flow that occurred in the winter of 2006. Site 3 was not visible as the river contained suspended sediment and was too swift and deep for safe wading.

3.2.2.4 Spawning dunes

There are several indications that bedload coarsening and mild channel incision has occurred in the evaluation area as result of sediment supply interruption and hydrologic regime alteration. Patterns of static conditions typical of rivers below dams are also present in the upper reach, albeit somewhat subdued. Static in this case pertains to bed stability with low potential for sediment transport. The upper reach has a distinctively coarser bed than the lower reach (see Appendix E), which is likely a result of the interruption of sediment supply from the upper basin, although this is confounded somewhat by the fact that the upper reach is more confined and thus has greater transport capacity. A prominent indicator of bed stability in the upper reach is the presence of spawning dunes that are the result of heavy use by spawning salmon (Figure 12). The spawning dunes can only be created and persist where no sediment transport is occurring.

3.3 Conclusion

Spawning gravel in the Lewis River is stable but limited. Modeling of the average annual sediment transport rate below Merwin Dam shows that transport of sediment is relatively low. The upper reach of the river has inherently less spawning gravel extent due to its bedrock confinement compared to the lower reach. The present day morphology of the river is most likely the legacy of the flood of record which occurred in 1933, modified by incremental vegetation encroachment and channel entrenchment since. It appears that no flood since the 1933 flood has had as profound an effect on the channel bed and overall reach morphology. Prevalent spawning dunes in the upper reach are evidence for spawning habitat limitation. Habitat limitation modeling indicates that habitat limitation is occurring in the upper reach, and that the present levels of escapement are probably representative of the available production capacity of Lewis River below Merwin Dam.

It is fortunate for salmon that the Lewis River channel downstream of Merwin Dam is useable to spawning Chinook salmon. The Sacramento River and Merced River in California are prime examples of how a river generally responds to depleted sediment supply and altered peak flow events following construction of dams. In the Sacramento and Merced rivers below their respective dams the bed has coarsened such that spawning habitat has become critically limited for endangered populations of Chinook salmon. Below River Mill Dam on the Clackamas River, Oregon, extreme bed coarsening has resulted in a bed that is bedrock or a layer of boulders over bedrock.

4 MONITORING PLAN

The spawning gravel monitoring plan will consist of two components. The first component is monitoring of stream discharge that reaches or exceeds a minimum discharge (termed spawning gravel monitoring discharge). The second component will consist of spawning habitat mapping in the spawning season following the year that the spawning gravel monitoring discharge occurs.

4.1 Minimum Discharge

The results of the EASI modeling (Section 2.5) indicate the daily average discharge at which incipient motion occurs at approximately 56,000 cfs for the upper and 42,000 cfs for the lower reach. We propose setting a spawning gravel monitoring discharge of 42,000 cfs (instantaneous discharge), which is approximately a 4-year flow event within the study reach.

4.2 Spawning Habitat Use Monitoring

Mapping of spawning habitat use in the upper reach will occur during the spawning season following the spawning gravel monitoring discharge. The methods used to map the spawning habitat will be similar to the approach used in the 2005 field effort (see Section 2.4). Very low escapement is required to saturate the available spawning habitat in the upper reach (Section 2.6), so in most years under-representation of available spawning habitat is a low risk.

Available spawning habitat will be mapped during the spawning season of 2006 to establish a benchmark for future monitoring. Three index sites will be mapped in detail to track future change, if any, in available spawning habitat as indicated by spawner use. High-resolution low-elevation aerial photography (LEAP) will be used to map usable gravel in 2006 and after a triggering monitoring discharge. The extent of spawning habitat loss which would trigger gravel augmentation will be determined in consultation with the ACC after 2006 and 2007 evaluations are completed.

5 GRAVEL AUGMENTATION STRATEGY

5.1 Spawning Gravel Augmentation Strategy Options

The general design guidelines for gravel augmentation, should it be required, may consist of one or a combination of the following two options:

- 1) An annual input of gravel equal to the average annual sediment transport rate for the upper reach, as determined by the final EASI modeling. The gravel will be introduced just below the dam, and the river will be allowed to naturally route the sediment from upstream to downstream.
- 2) Site-specific augmentation of gravel in areas with documented loss of spawning gravel. The volume and extent of gravel to be added will be determined on a case-by-case basis in the event gravel augmentation is required.

Option 1, introducing the sediment just below the dam and allowing the river to route it downstream, has three advantages. First, there is road access to the river immediately below the dam, making delivery relatively easy, with no need for heavy equipment to operate within the stream channel itself. Secondly, the section of the river immediately below the dam (RM 19.5 to RM 19.35) is not a key spawning area, so the addition of gravel will have low impact on spawning habitat. Thirdly, allowing the river to route the sediment will allow coarsened areas to fill in and be shaped as they would under natural conditions, eliminating the need for more costly and questionable engineering solutions. The potential disadvantage of this option is that if substantial channel incision has occurred, routing of the added gravel to critical downstream spawning areas may take many years because high flows with the capacity for transporting sediment under these conditions are relatively rare. In the interim, spawning habitat limitations may continue to substantially limit salmon production. This could be remedied by immediate addition of gravel to the channel, which is described below.

Option 2 would more immediately replace local gravels lost during the last flood event; however, it is difficult to determine the extent to which gravel loss has occurred and thus the amount to add to the channel. The main problem with this approach is that access to the channel to add gravel may be difficult or impossible in certain reaches, particularly in the gorge of the upper reach. Gaining access through private property may further complicate implementation of this option.

A third option is the immediate addition of gravel at RM 19.3 to create a spawning riffle and enhance available spawning habitat. This option has three advantages. In the near term, creating a new spawning riffle in the uppermost spawning area of the upper reach would increase spawning habitat quantity and quality in one of the most heavily used spawning areas, which already exhibits evidence of density-dependent habitat limitations (Section 3.1). In addition, while the new spawning riffle would be designed to be stable at most high flows, in the event of a very large flood event, it could act as a source of gravel for replenishing areas downstream that have lost gravel. Access to the upper reach is good and heavy equipment impacts to existing spawning habitat would be negligible. A third and most important advantage is that the gravel remaining within the reach after a high flow event could be used to indicate whether more gravel augmentation is needed. The main disadvantage of this option is that it requires equipment and cost outlay in the near term.

5.2 Spawning Gravel Augmentation Monitoring Plan Design and Review

The three options for gravel augmentation correspond to different philosophies: option 1 assumes that future gravel losses will be minor and that the purpose of augmentation is to maintain existing habitat;

option 2 is more expensive but would increase spawning habitat quality and quantity for Chinook salmon; and option 3 preemptively increases spawning habitat and provides insurance against potential future losses. We believe option 3 can accomplish the objective with relatively small risk of damaging the habitat and reasonable budget.

The approach presented here is aimed at maintaining current gravel storage capacity and should be effective if the channel downstream of the dam has incised to some degree, but not enough to cause substantial loss of spawning gravels. Before gravel augmentation occurs, however, a detailed plan would be developed and submitted for review. The detailed design should contain at minimum the following components: a bulk particle size analysis of the present river bed, a gravel particle size distribution for gravel to be added based on native bulk samples and desired outcome, and a risk evaluation of potential effects of gravel augmentation. If an annual gravel augmentation plan is implemented it should be reviewed every 10 years (up to three times during the license term) to determine if any adjustments are needed. This review may result in a termination, decrease, or increase of the amount of gravel added annually.

6 2006 AND 2007 FIELDWORK

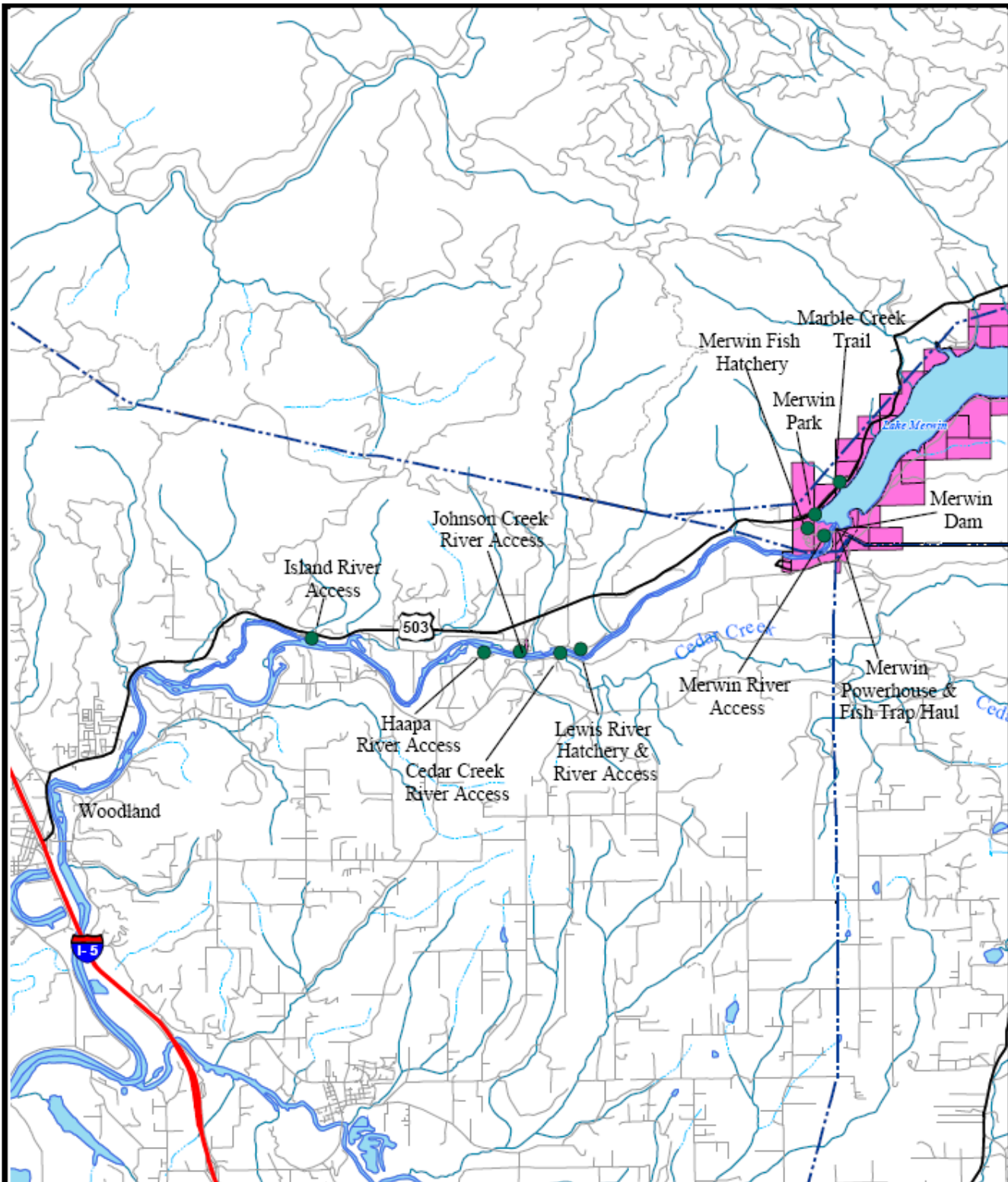
Field work to be completed in 2006 and 2007 will consist of monitoring the movement and replacement of tracer gravels (if needed) after sufficiently high flow events, detailed channel slope measurements, and detailed mapping of spawning habitat use by Chinook salmon during the peak spawning season.

7 LITERATURE CITED

- Bio-Analyst, EDAW, Historical Research Associates, Hardin-Davis, Mason Bruce & Girard, Meridian Environmental, Mobrand Biometrics, Montgomery Watson Harza, Northwest Hydraulic Consultants, Washington Department of Fish and Wildlife, and Watershed GeoDynamics. 2003. Final Licensee's 2001 technical study status reports for the Lewis River Hydroelectric Projects. FERC No. 935, 2071, 2111, 2213. Prepared for PacifiCorp, Portland, Oregon and Public Utility District No. 1 of Cowlitz County, Longview, Washington.
- Buffington, J. M., and D. R. Montgomery. 1999. A procedure for classifying textural facies in gravel-bed rivers. *Water Resources Research* 35: 1903-1914.
- Hawkins, S. 1998. Results of sampling the Lewis River natural spawning fall Chinook population in 1997. Washington Department of Fish and Wildlife, Fish Program - Southwest Region 5, Vancouver, Washington.
- Hawkins, S. 2006. Personal communication. Wildlife Biologist, Washington Department of Fisheries and Wildlife, Vancouver, Washington. 28 May.
- Hayes, J. W. 1987. Competition for spawning space between brown (*Salmo trutta*) and rainbow trout (*S. gairdneri*) in a lake inlet tributary, New Zealand. *Canadian Journal of Fisheries and Aquatic Sciences* 44: 40-47.
- Leopold, L. B., M. G. Wolman, and J. P. Miller. 1964. *Fluvial processes in geomorphology*. W. H. Freeman and Company, San Francisco, California.
- Lestelle, L. C., L. E. Mobrand, J. A. Lichatowich, and T. S. Vogel. 1996. *Applied ecosystem analysis--a primer*. Prepared by Mobrand Biometrics, Inc., Vashon Island, Washington for Bonneville Power Administration, Portland, Oregon.
- Ligon, F. K., W. E. Dietrich, and W. J. Trush. 1995. Downstream ecological effects of dams: a geomorphic perspective. *BioScience* 45: 183-192.
- McNeil, W. J. 1964. Redd superimposition and egg capacity of pink salmon spawning beds. *Journal of the Fisheries Research Board of Canada* 21: 1385-1396.
- Parker, G. 1990. Surface-based bedload transport relation for gravel rivers. *Journal of Hydraulic Research* 28: 417-436.
- Rogers, D. W. 1973. King salmon (*Oncorhynchus tshawytscha*) and silver salmon (*Oncorhynchus kisutch*) spawning escapement and spawning habitat in the upper Trinity River, 1970. Anadromous Fisheries Branch Administrative Report No. 73-10. California Department of Fish and Game, Region 1.
- Sommer, T., D. McEwan, and R. Brown. 2001. Factors affecting Chinook salmon spawning in the lower Feather River. Pages 269-297 in R. L. Brown, editor. *Contributions to the biology of Central Valley salmonids*. Fish Bulletin 179: Volume 1. California Department of Fish and Game, Sacramento.
- Stillwater Sciences. 2002. Review of draft report on Lewis River Geomorphology Study (updated version). Technical Memorandum to F. K. Shrier, PacifiCorp, Portland, Oregon from P. Downs, Y. Cui, and C. Braudrick, Stillwater Sciences, Berkeley, California. 19 December.

TID/MID (Turlock Irrigation District and Modesto Irrigation District). 1992. Lower Tuolumne River spawning gravel availability and superimposition. Appendix 6 to Don Pedro Project Fisheries Studies Report (FERC Article 39, Project No. 2299). *In* Report of Turlock Irrigation District and Modesto Irrigation District Pursuant to Article 39 of the License for the Don Pedro Project, No. 2299. Vol. IV. Prepared by EA Engineering, Science, and Technology, Lafayette, California.

Wolman, G. M. 1954. A method of sampling coarse river-bed material. *Transactions of the American Geophysical Union* 35: 951-956.



<p>PACIFICORP</p> <p>Public Utility District No. 1 of Cowlitz County</p> <p>January 23, 2004 c:\property_management\GIS\Geodatabase\MXD\client\MarkStenberg\03-57\mxd\PDEA_map_ah2.mxd</p>	<p>Legend</p> <ul style="list-style-type: none"> PacifiCorp Ownership CCPUD Ownership PacifiCorp FERC Boundary CCPUD FERC Boundary Transmission Lines <p>Project Facilities</p> <ul style="list-style-type: none"> New Existing
<p>Lewis River Hydroelectric Projects Alternative A FERC No. 935, 2071, 2111, 2213 Sheet 1 of 4 Figure 2.2-1</p> <p>0 1 2 Miles 0 1 2 Kilometers</p> <p style="text-align: center;">N</p>	

Figure 1. Location map of the Evaluation Area in southwestern Washington (taken from WTS-3 study results).



Figure 2. Example of tracer gravel grid.

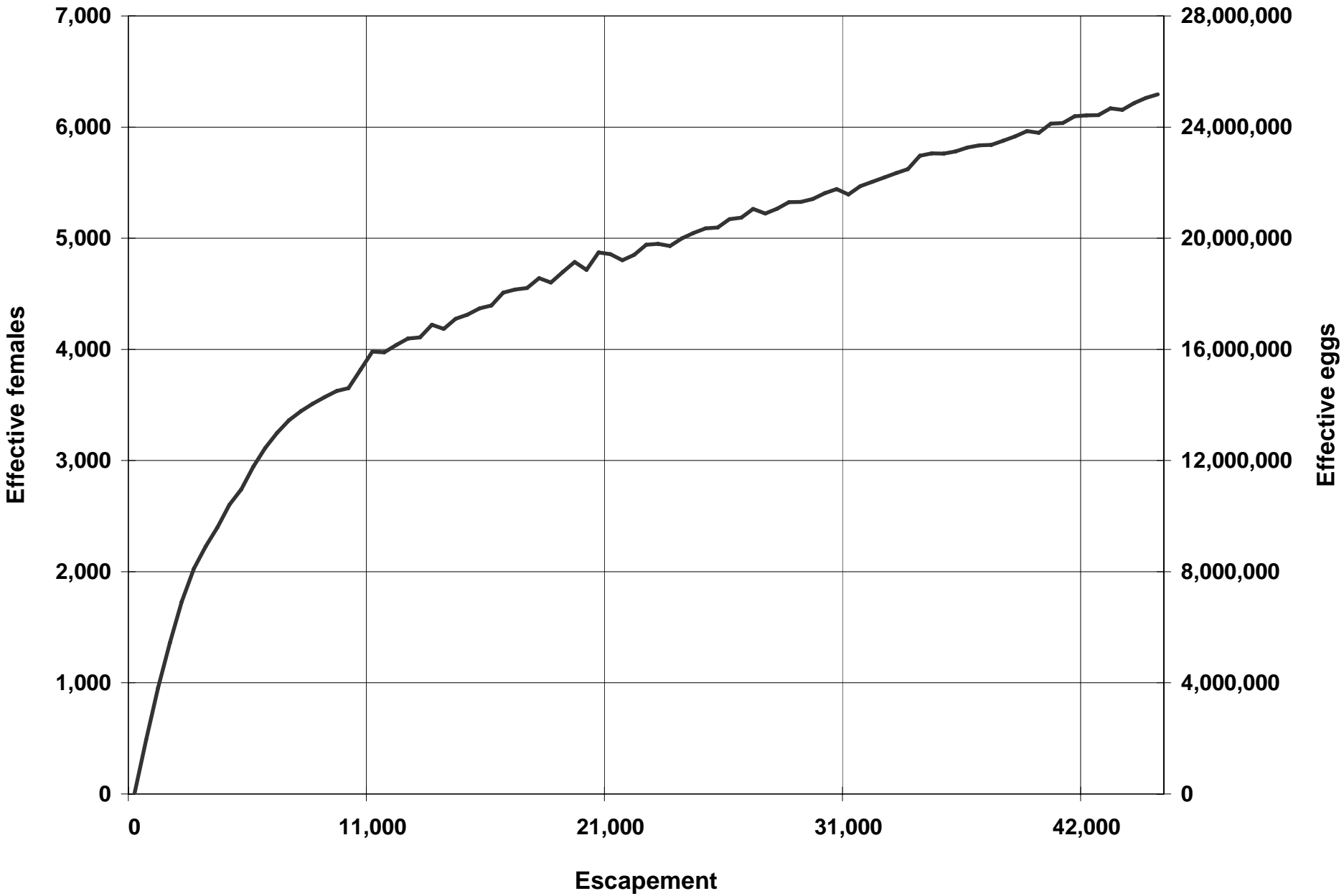


Figure 3. Chinook salmon effective females and effective eggs versus escapement from ESCAPE output.



Lewis River Tile 1 - Spawning Area Map

- Pebble counts
- Spawning areas

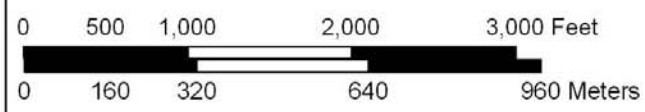
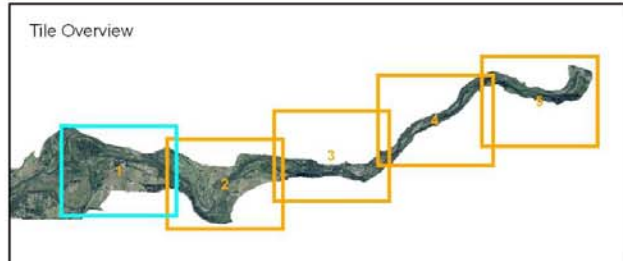


Figure 4a. Spawning habitat map, Tile 1.



Lewis River Tile 2 - Spawning Area Map

- Pebble counts
- Spawning areas

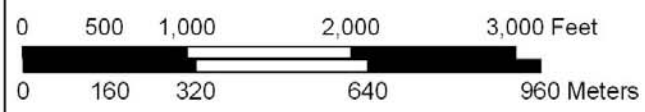
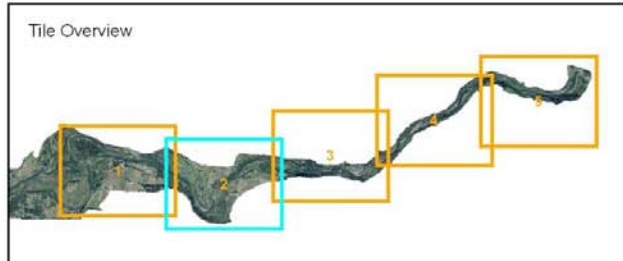


Figure 4b. Spawning habitat map, Tile 2.



Lewis River Tile 3 - Spawning Area Map

- Pebble counts
- Spawning areas

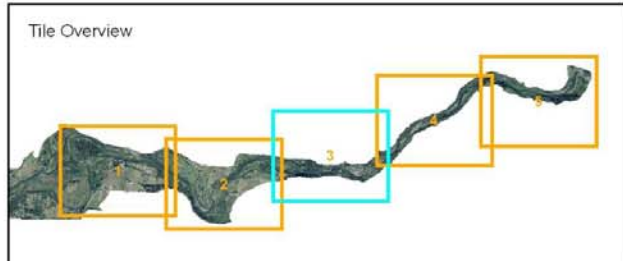
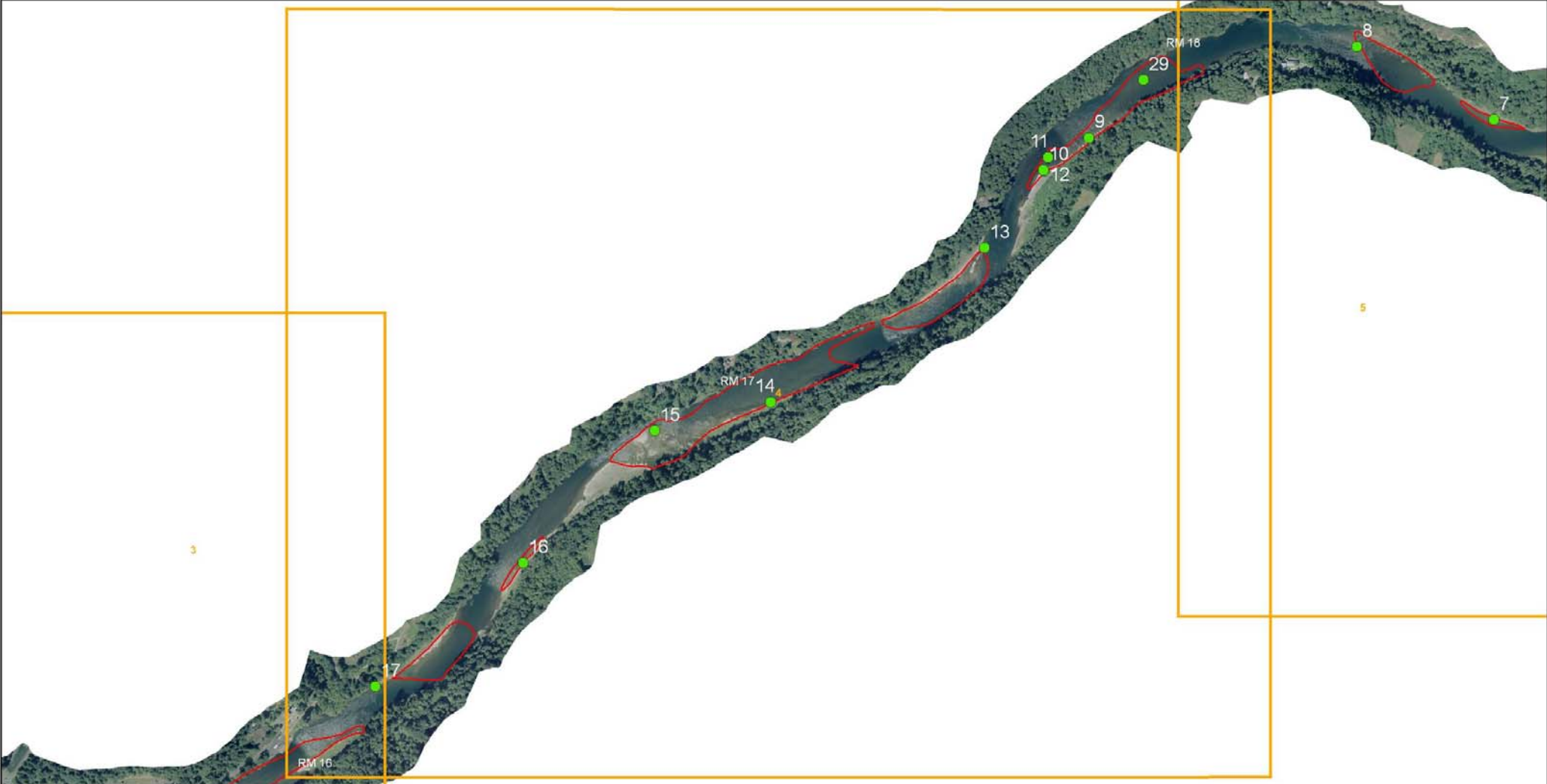
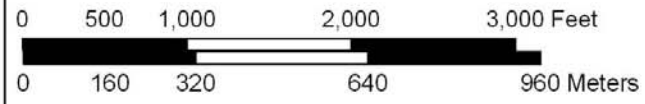
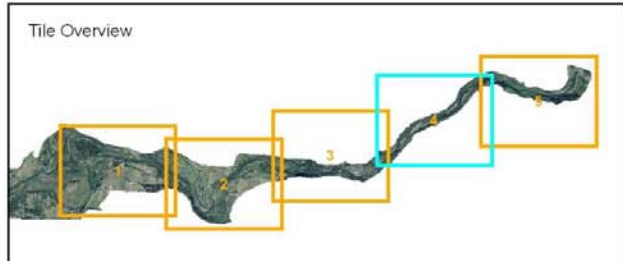


Figure 4c. Spawning habitat map, Tile 3.



Lewis River Tile 4 - Spawning Area Map

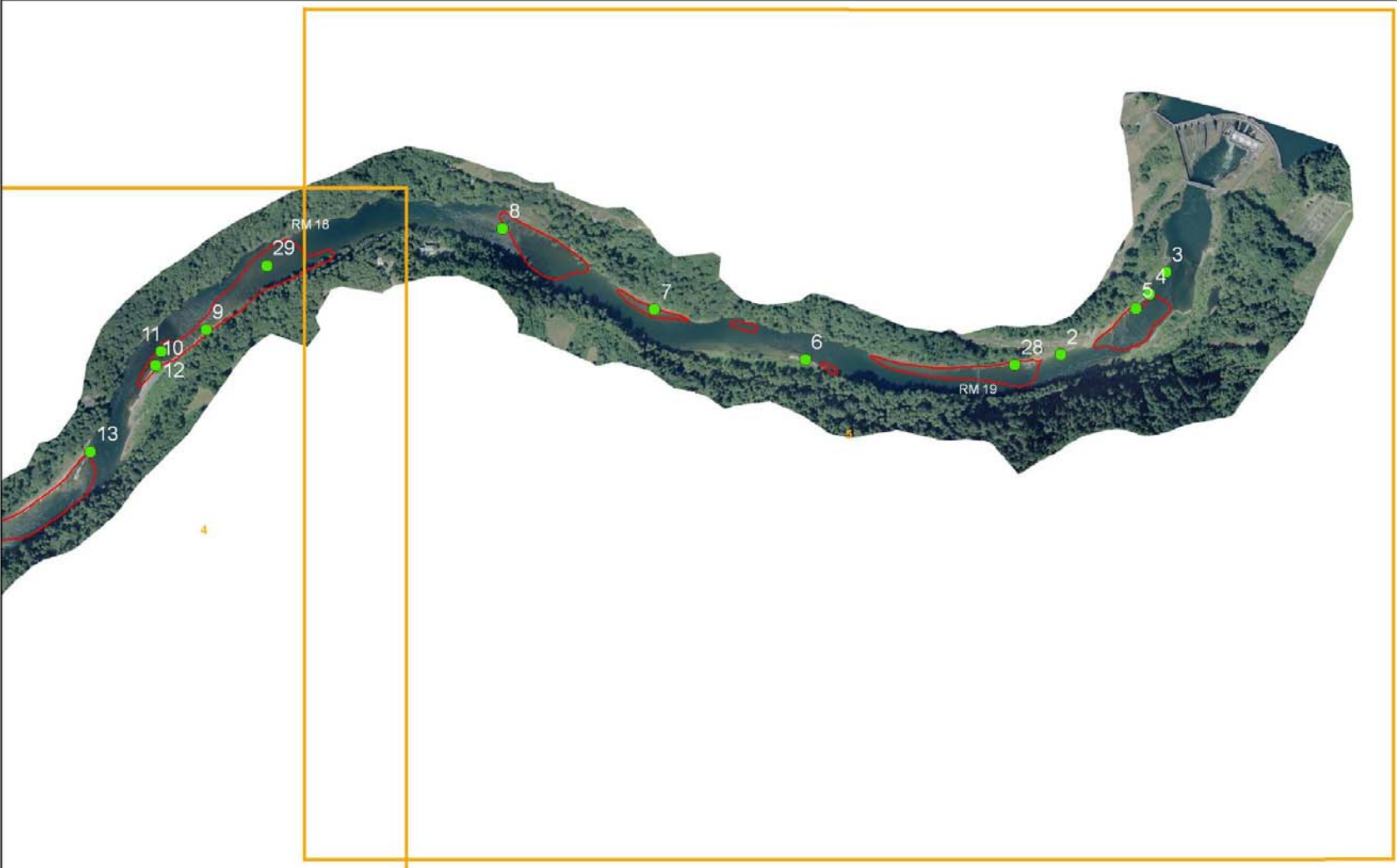
- Pebble counts
- Spawning areas



← Flow Direction

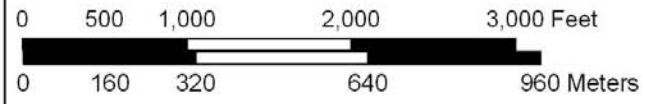
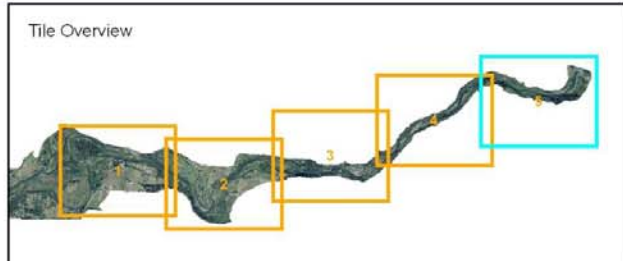


Figure 4d. Spawning habitat map, Tile 4.



Lewis River Tile 5 - Spawning Area Map

- Pebble counts
- Spawning areas



← Flow Direction



Figure 4e. Spawning habitat map, Tile 5.

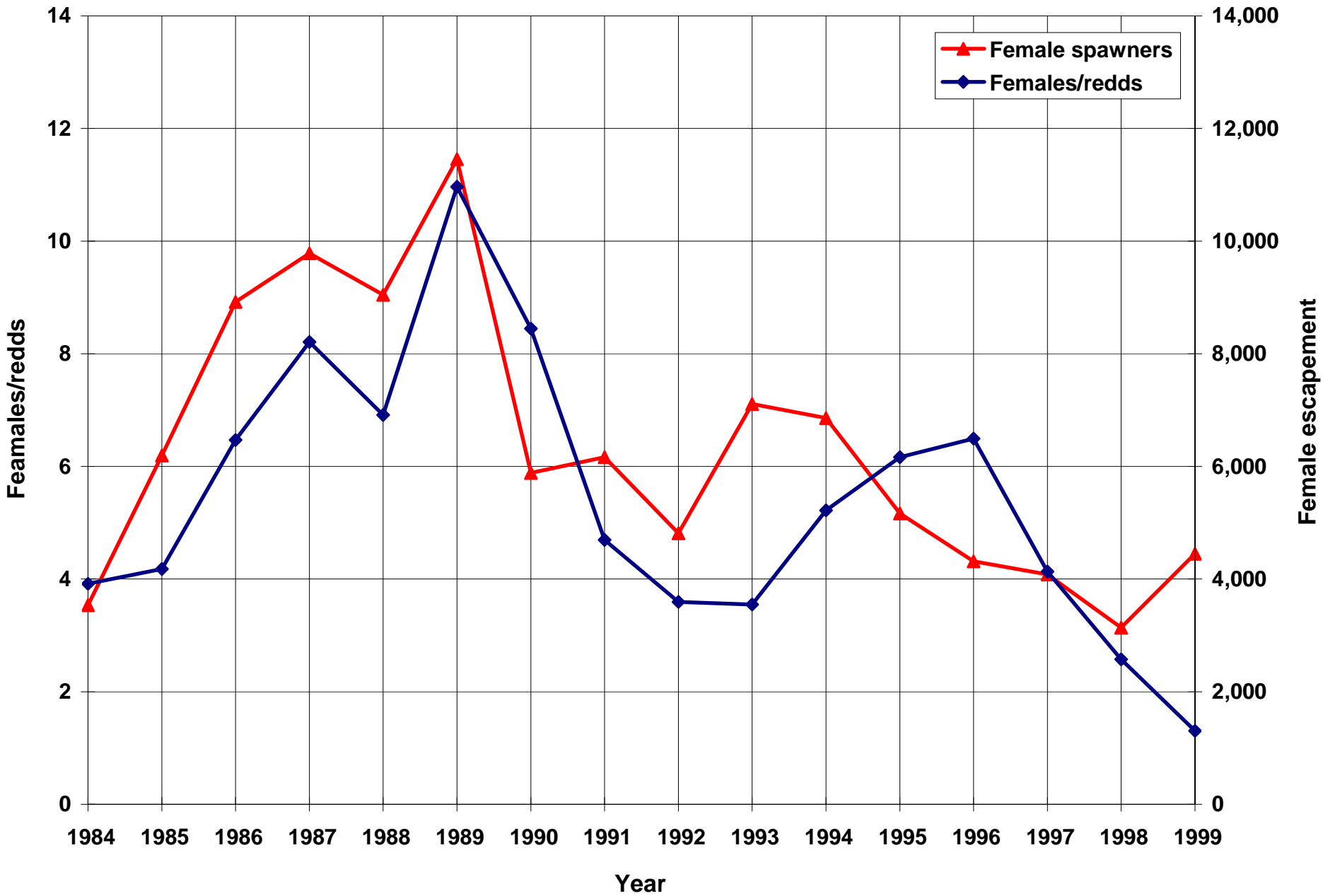


Figure 5. Female spawner escapement and females to redds ratio in the Lewis River from 1984 to 1999.

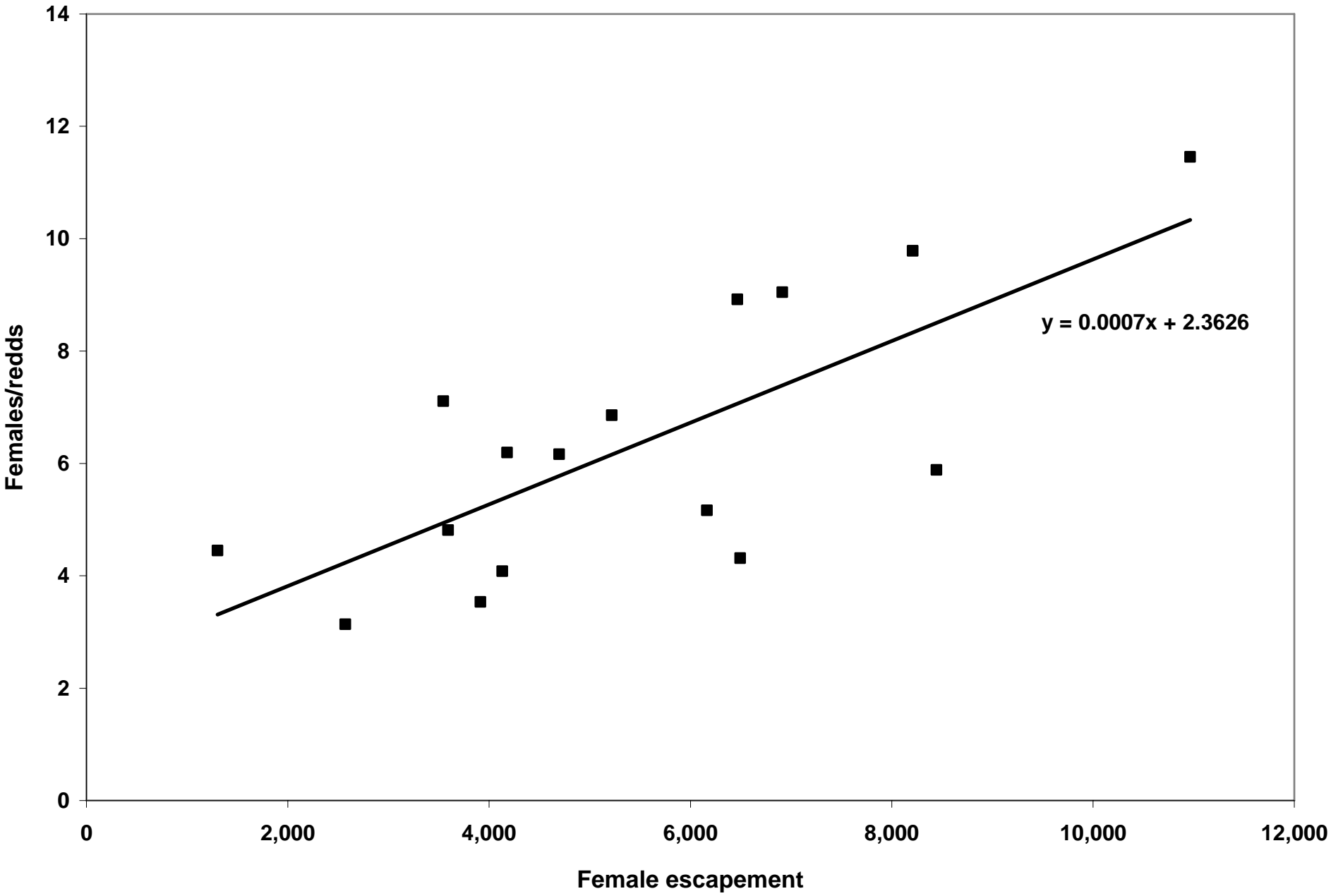


Figure 6a. Females to redds ratio versus female escapement in the Lewis River based on WFDW escapement estimates from 1984 to 1999.

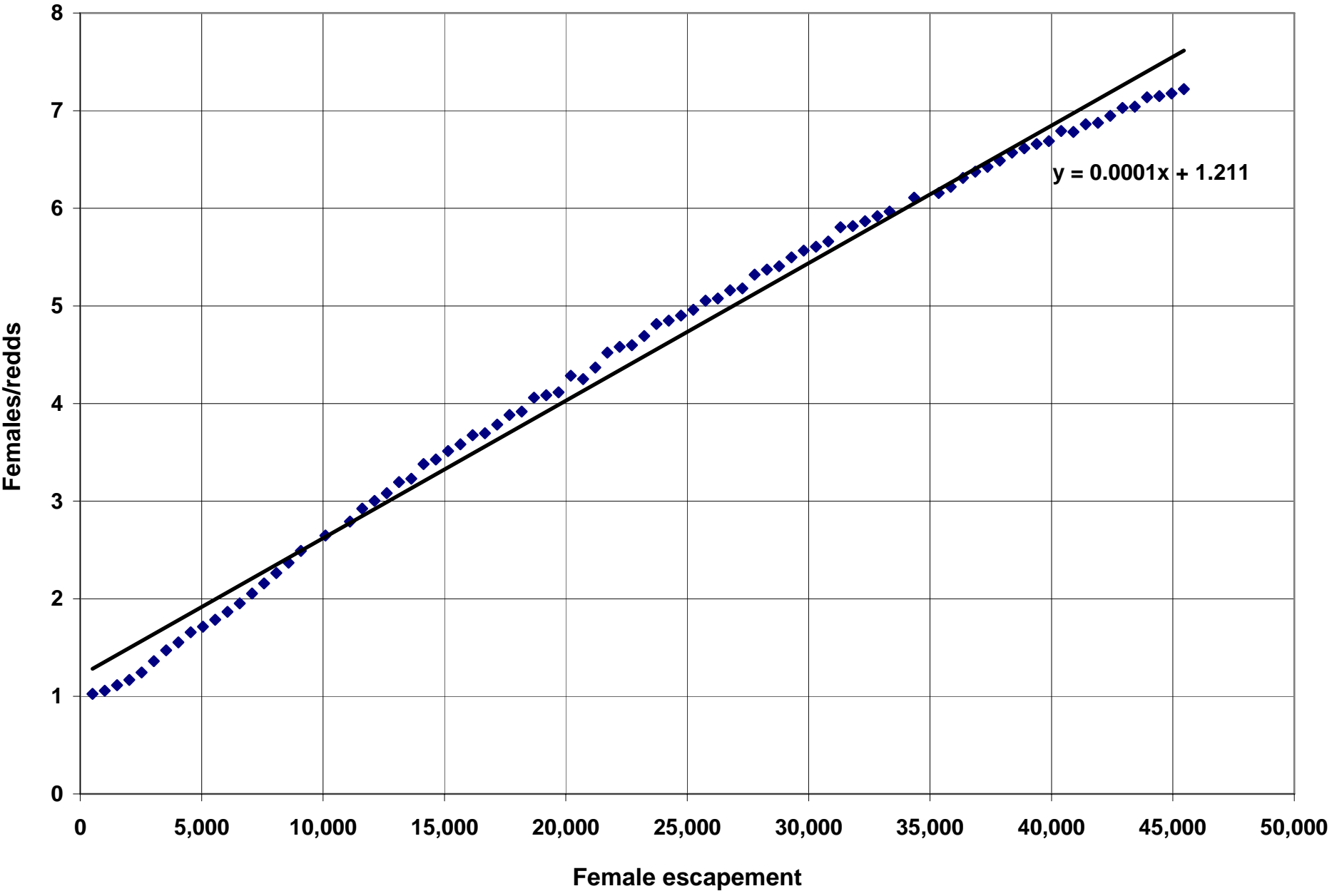


Figure 6b. Females to redds ratio versus female escapement in the Lewis River based on ESCAPE model output.

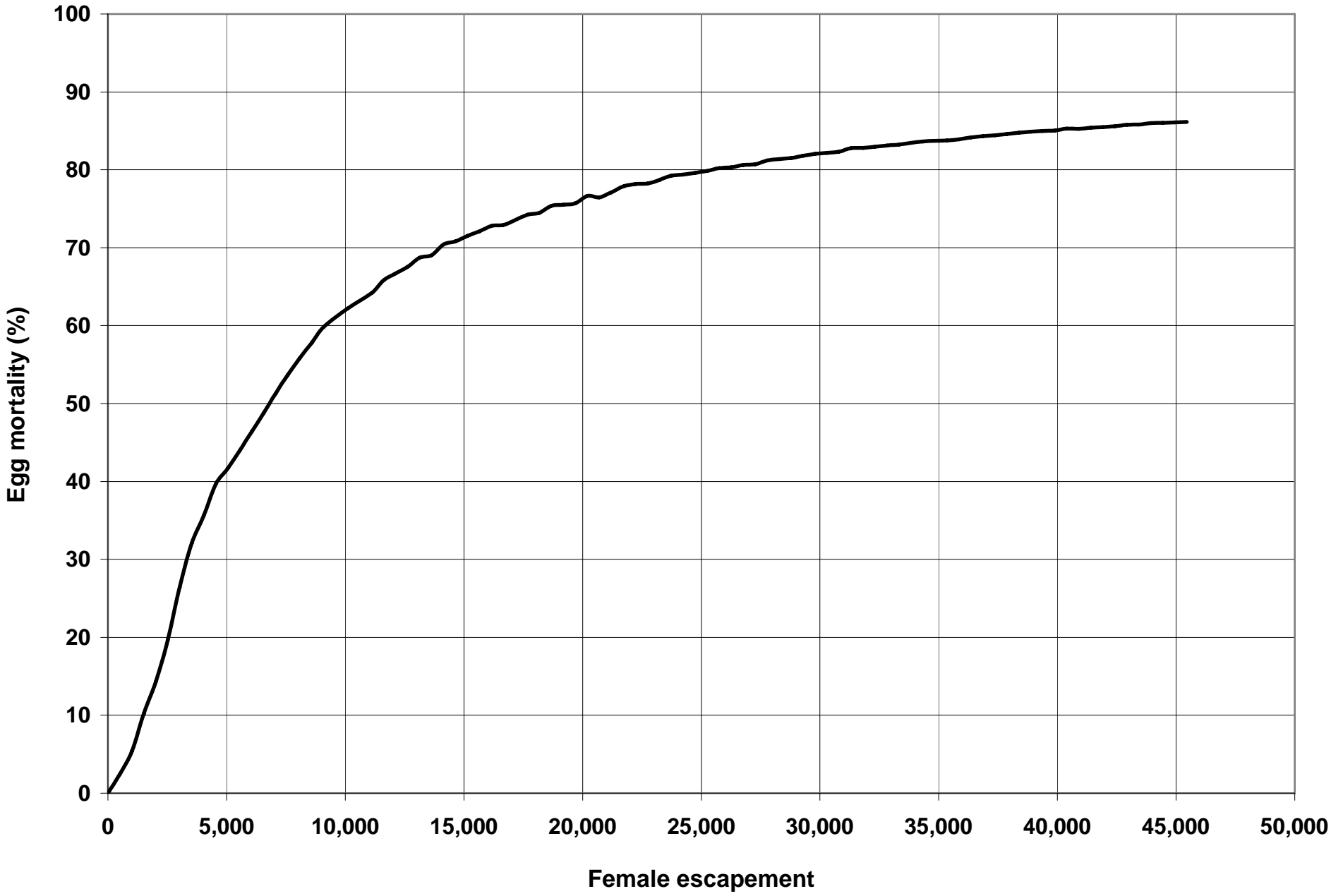
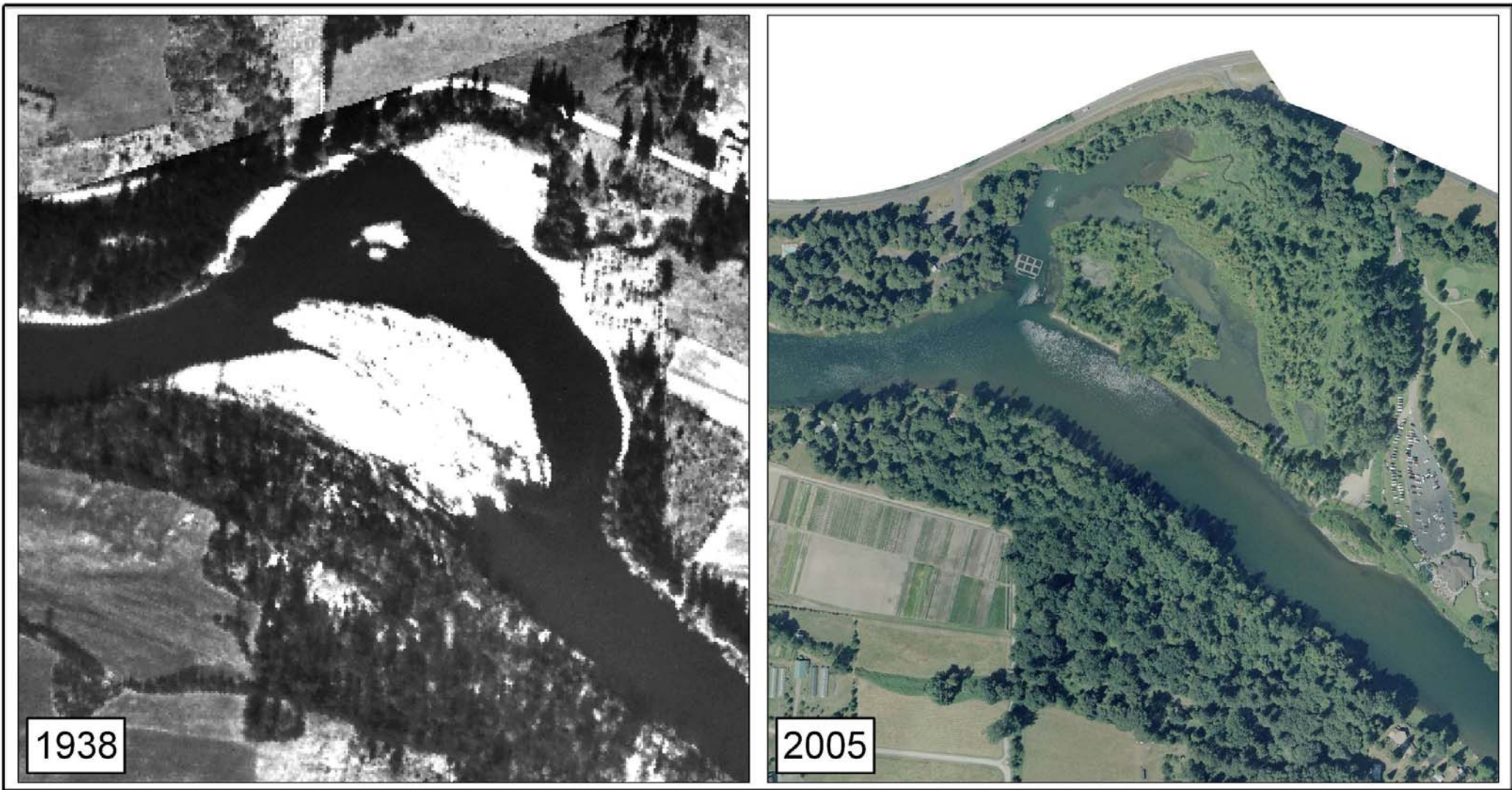


Figure 7. Chinook egg mortality versus female escapement from ESCAPE output.



**Side by side comparison of gravel bars
between 1938 and 2005 aerial photos**

Map 1 of 8

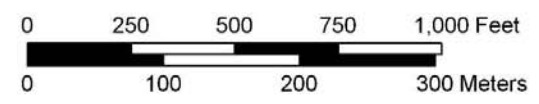
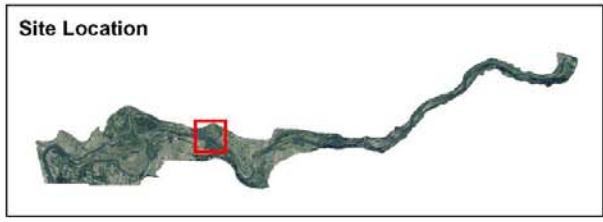
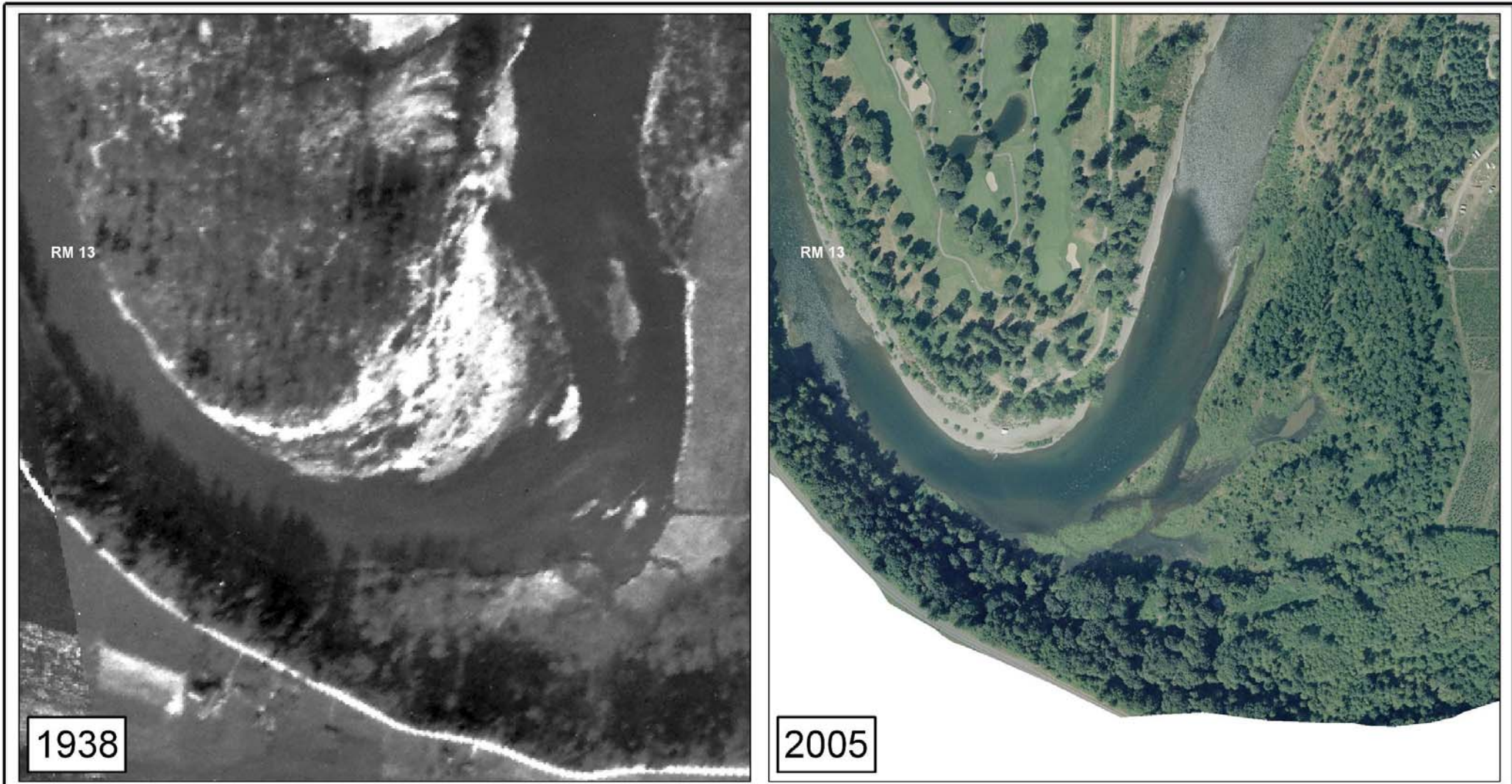


Figure 8a. Comparison of gravel bars in the Lewis River downstream of Merwin Dam between 1938 and 2005, Map 1.

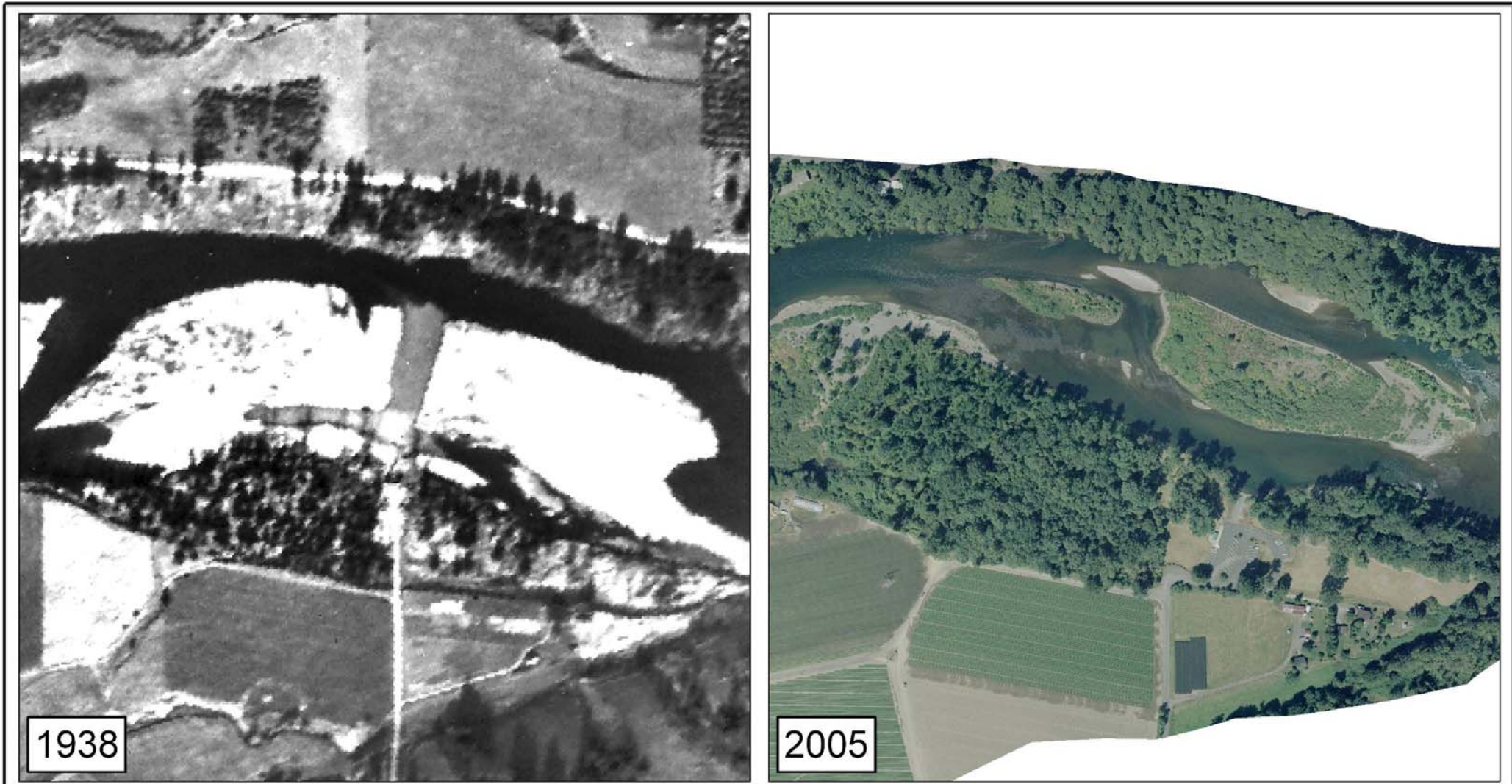


Side by side comparison of gravel bars between 1938 and 2005 aerial photos

Map 2 of 8



Figure 8b. Comparison of gravel bars in the Lewis River downstream of Merwin Dam between 1938 and 2005, Map 2.



Side by side comparison of gravel bars between 1938 and 2005 aerial photos

Map 3 of 8

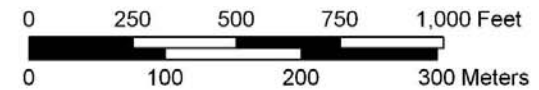
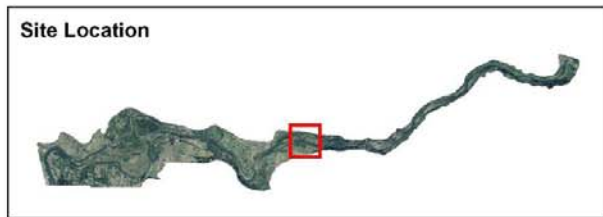
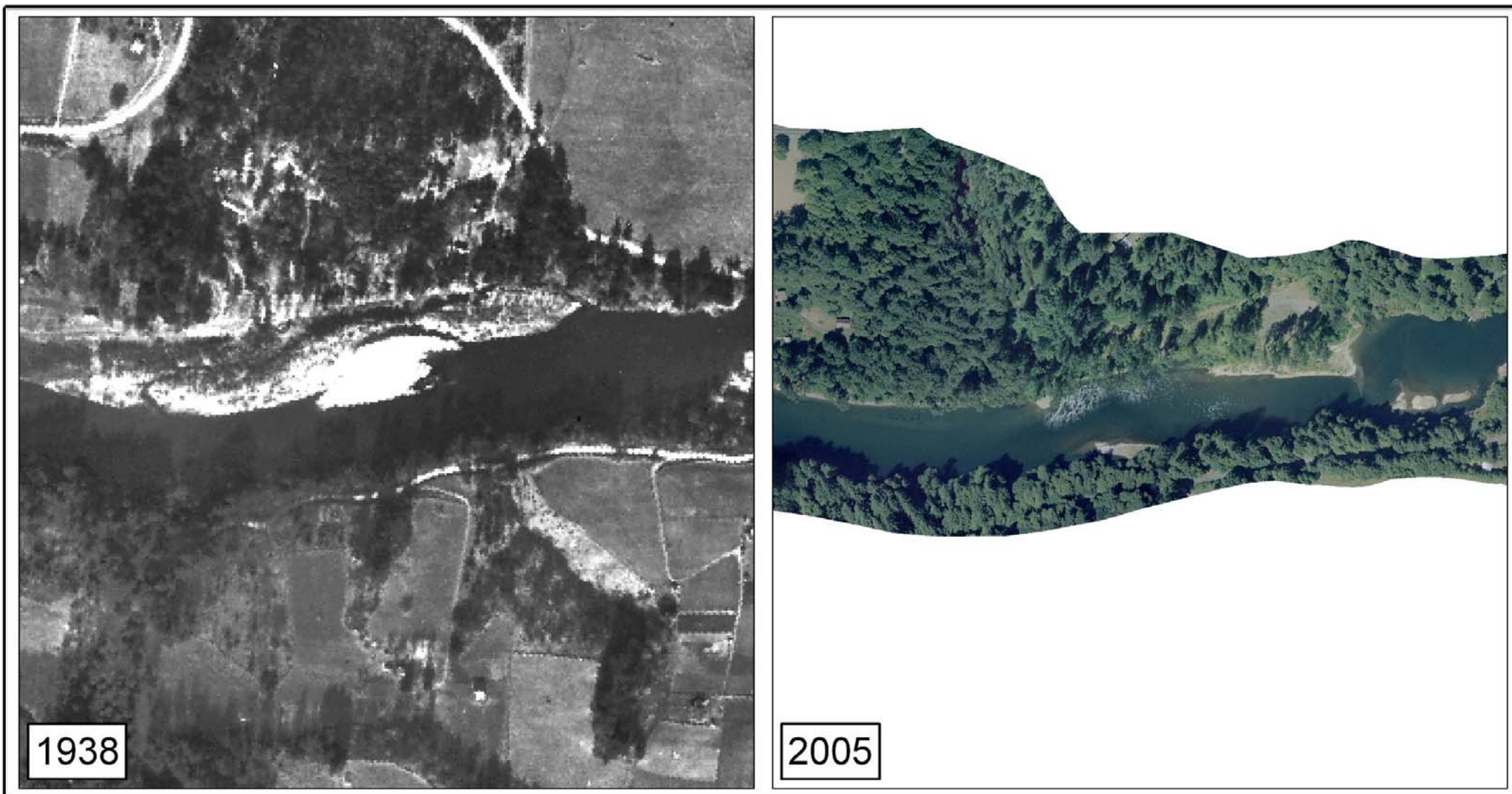


Figure 8c. Comparison of gravel bars in the Lewis River downstream of Merwin Dam between 1938 and 2005, Map 3.



Side by side comparison of gravel bars between 1938 and 2005 aerial photos

Map 4 of 8

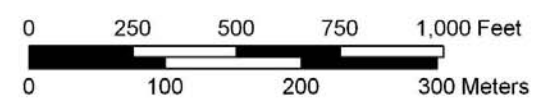
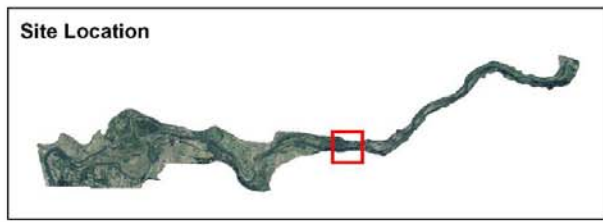


Figure 8d. Comparison of gravel bars in the Lewis River downstream of Merwin Dam between 1938 and 2005, Map 4.



Side by side comparison of gravel bars between 1938 and 2005 aerial photos

Map 5 of 8

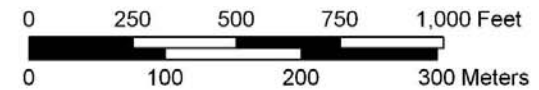
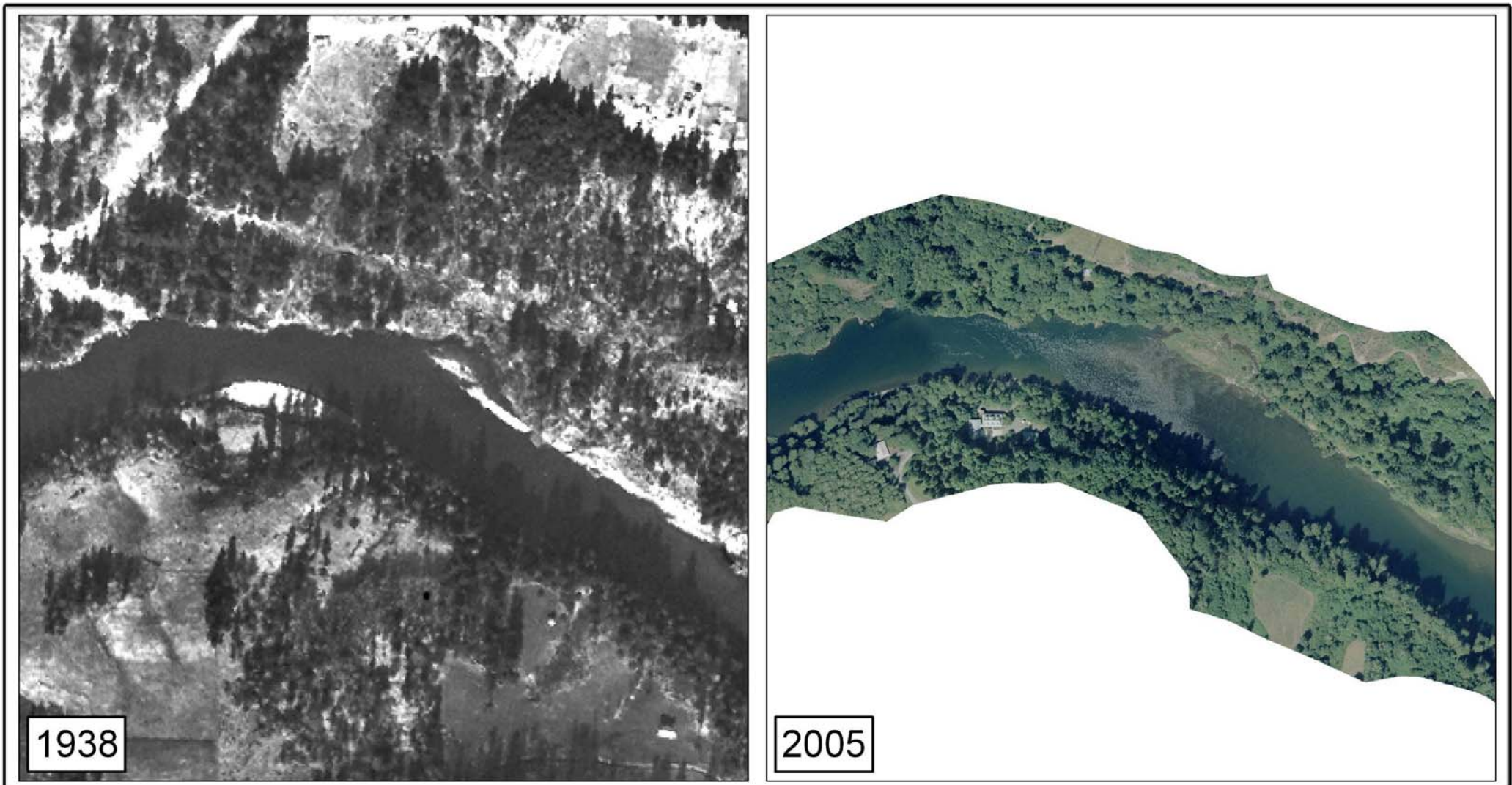


Figure 8e. Comparison of gravel bars in the Lewis River downstream of Merwin Dam between 1938 and 2005, Map 5.



1938

2005

Side by side comparison of gravel bars between 1938 and 2005 aerial photos

Map 6 of 8

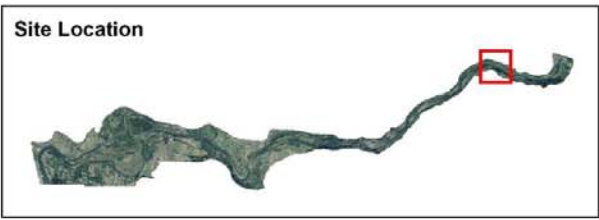
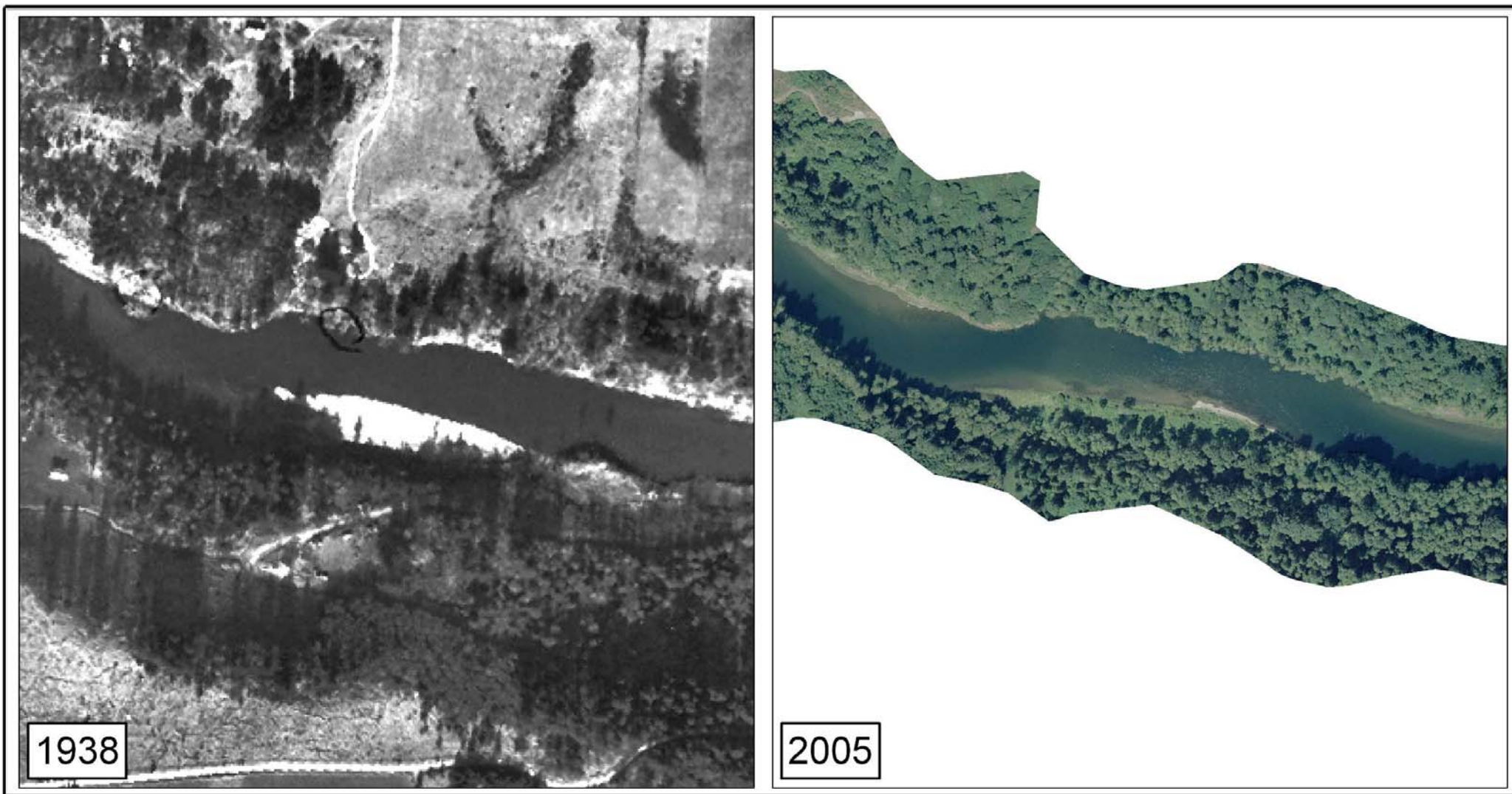


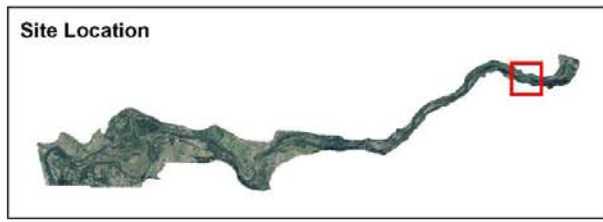
Figure 8f. Comparison of gravel bars in the Lewis River downstream of Merwin Dam between 1938 and 2005, Map 6.



1938

2005

**Side by side comparison of gravel bars
between 1938 and 2005 aerial photos**
Map 7 of 8



Flow Direction ←

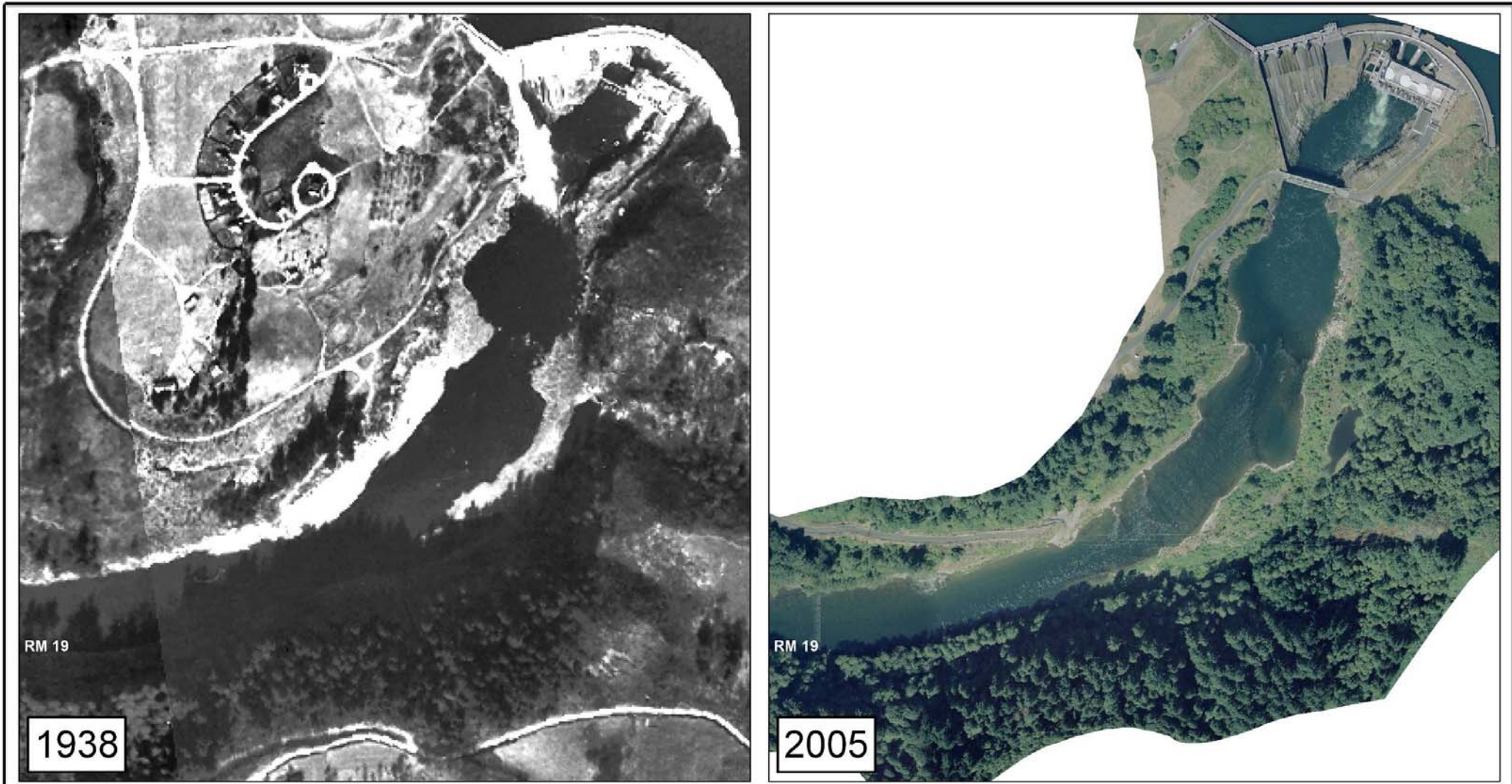


1:3,600



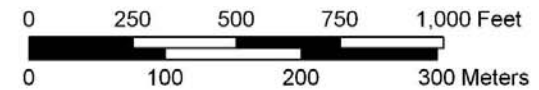
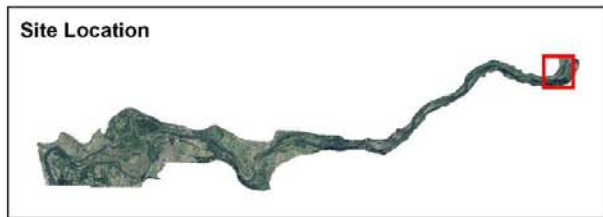
Stillwater Sciences

Figure 8g. Comparison of gravel bars in the Lewis River downstream of Merwin Dam between 1938 and 2005, Map 7.



Side by side comparison of gravel bars
between 1938 and 2005 aerial photos

Map 8 of 8



Flow Direction
←



1:3,600



Stillwater Sciences

Figure 8h. Comparison of gravel bars in the Lewis River downstream of Merwin Dam between 1938 and 2005, Map 8.



Figure 9. Scarp on static point bar at RM 19.2 on the north bank of the Lewis River.



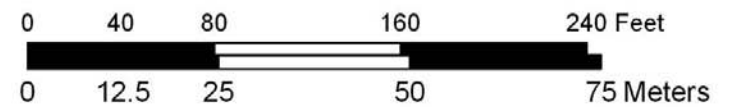
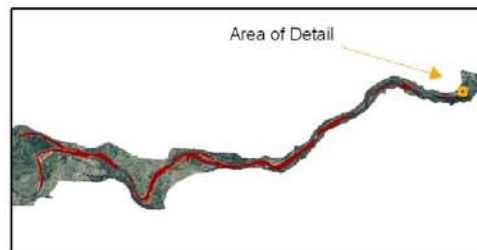
Figure 10. Static point bar with scarp with riparian vegetation.



Figure 11. Riparian forest at RM 15.2 on south bank of the Lewis River.



Lewis River Facies map - Detail of Spawning Dunes



← Flow Direction



Stillwater Sciences

Figure 12. Detail of spawning dunes in WDFW spawning Index Reach 1.

Appendices

Appendix A

Background information on Project relicensing

The Lewis River Hydroelectric Projects consist of the Merwin Project (Project No. 935), Yale Project (Project No. 2071), Swift No. 2 Project (Project No. 2213), and Swift No. 1 Project (Project No. 2111) (each individually referred to as a “Project” and collectively as the “Projects”) and associated powerhouses, transmission facilities, recreational facilities, hatcheries, reservoirs, canals, and lands within the Projects’ Boundaries and wildlife lands managed outside the Project Boundaries. PacifiCorp owns the Merwin Yale and Swift No. 1 Project, while Cowlitz PUD owns the Swift No. 2 Project (the combined Projects of Swift No. 1 and Swift No. 2 are referred to collectively as the “Swift Projects”). Construction of the Projects began with the Merwin Dam in 1929 and was completed with the construction of Swift No. 1 and Swift No. 2 ending in 1958. The Federal Power Commission issued the first license for Merwin on November 29, 1929, which expired on November 29, 1979. That license was renewed on October 6, 1983 and was originally due to expire on April 30, 2009 but was accelerated by a Commission Order and now expires on April 30, 2006. The original license for Yale was issued on April 24, 1951 and expired on April 30, 2001. The original license for Swift No. 1 was issued on May 1, 1956 and expires on April 30, 2006. The original license for Swift No. 2 was issued on November 29, 1956, effective May 1, 1956, and expires on April 30, 2006.

In January 1999, PacifiCorp and Cowlitz PUD filed a request with the Commission for approval of the use of the Commission’s Alternative Licensing Procedures and for the simultaneous and coordinated processing of the license applications for all four Projects. In April 1999, the Commission approved this request and issued an order accelerating the Merwin license expiration. An application to relicense the Yale Project was submitted to the Commission in 1999. The Commission granted PacifiCorp’s request that processing of the Yale license application be deferred until the applications for Merwin, Swift No. 1, and Swift No. 2 were filed on or before April 30, 2004. The Parties anticipate concurrent environmental review of all four Projects. On April 29 and 30, 1999, PacifiCorp and Cowlitz PUD initiated the collaborative process with a public meeting. A Memorandum of Agreement and Communications Protocol among the Parties was developed for the collaborative process.

Appendix B

Section 7.2 from the Lewis River Hydroelectric Projects
Settlement Agreement

7.2 Spawning Gravel Study and Gravel Monitoring and Augmentation Plan

- a. Contracting with Consultant. Within six months after the Effective Date, PacifiCorp shall contract with a qualified consulting firm, selected in Consultation with the ACC, to develop and implement a spawning gravel study and, on the basis of the study results, to develop a gravel monitoring and augmentation plan.
- b. Draft Study Plan. The general scope of the study is described on attached Schedule 7.2. PacifiCorp shall cause the consultant to submit a draft study plan to the ACC for review upon Issuance of the New License for the Merwin Project. In addition to any review by the ACC, PacifiCorp may provide input to the consultant when it is developing the plan, as long as PacifiCorp provides the ACC, prior to the ACC's 60-day review period, with the consultant's original drafts and PacifiCorp's comments. The ACC may comment on the draft study plan within 60 days after receipt.
- c. Finalizing and Completing the Study and Preparing Study Report. PacifiCorp shall direct the consultant to finalize the study plan within 90 days after submission of the draft to the ACC, to complete the study, and to deliver a draft study report to the ACC. Prior to the submission of the draft study report to the ACC, PacifiCorp may provide input to the consultant, so long as PacifiCorp provides the consultant's original drafts of the study report and PacifiCorp's comments to the ACC along with the draft study report. The ACC shall have 60 days to comment on the draft study report. PacifiCorp shall consult with the ACC on the draft study report. PacifiCorp shall direct the consultant to finalize the study report within 120 days after submission of the draft study report to the ACC. The study report will include the results of the study and a gravel monitoring and augmentation plan that describes gravel monitoring, the mechanism to determine when gravel augmentation will occur, and how gravel augmentation shall occur if the monitoring shows augmentation is necessary, during the term of the New License for the Merwin Project.
- d. Implementation of Gravel Monitoring and Augmentation Plan. PacifiCorp shall implement the gravel monitoring and augmentation plan. The monitoring and augmentation plan shall not require any augmentation that would increase the gravel levels beyond those existing on the date of the consultant's study.

Appendix C

Schedule 7.2 from the Lewis River Hydroelectric Projects
Settlement Agreement

Schedule 7.2: Scope of Spawning Gravel Study

Study objective: (1) Provide a monitoring program to provide a reliable basis to judge present conditions and changes over time in spawning habitat area in the Lewis River below Merwin Dam, and (2) Provide a means to determine when spawning gravel supplementation efforts to preserve or expand such areas is warranted.

An independent consultant will perform the following tasks:

Task 1 – Develop a long-term monitoring program to assess the retention of gravel of suitable size for salmon spawning in areas downstream of Merwin Dam. This evaluation should evaluate present spawning areas and areas that may be used once salmon populations are recovered. The spatial extent of the evaluation will be based on a geomorphic analysis of how far downstream the effects of reduced gravel supply on spawning habitat might extend. The goal is to find a methodology that (1) quantifies the amount of suitable gravel, (2) indicates where there is a change, and (3) is repeatable. Assessments would occur annually for the first 3 years. Follow up assessments will occur following flood events. The consultant will determine the recurrence interval of floods necessary to trigger an assessment.

Task 2 – Develop a scheme (stating assumptions and rationale) to determine when gravel augmentation would need to occur. In developing this scheme, the consultant should consider the habitat requirements of a recovered population rather than the current population, subject to the limitations in Section 7.2 (d) of the Settlement Agreement.

Task 3 – Propose a gravel augmentation program that addresses the quality of gravel to be augmented, the timing of the augmentation, and the methods to be used. The program shall be flexible enough to allow for incorporation of new technology or knowledge into the means by which gravel augmentation could occur.

Reporting

Study plan development and implementation schedule to be set forth in Settlement Agreement. A draft report will be sent out to parties for review. Prepare a final report, incorporating comments from interested parties.

Appendix D

EASI sediment transport model

8 DESCRIPTION OF EASI MODEL FORMULATION

The surface based bedload equation of Parker (1990a and 1990b) is expressed for wide rectangular channel for which channel geometry can be expressed as a channel width. The equation is modified for the Estimate of Adversary Sequence Interruption (EASI) program so that it can also handle a given cross section. Details of the surface based bedload equation of Parker can be found in the original references (Parker 1990a and 1990b). Here only the most essential part of the Parker equation is presented so that we can discuss how the equation is modified and implemented in the EASI program.

The surface based bedload equation of Parker (1990a and 1990b) for a wide rectangular channel is as follows,

$$\frac{RgQ_G p_i}{Bu_*^3} = \alpha F_i G \left[\omega \phi_{sgo} \left(\frac{\overline{D}_i}{D_{sg}} \right)^{-\beta} \right] \quad (\text{Equation A-1})$$

Where R denotes the submerged specific gravity of sediment; g denotes the acceleration of gravity; Q_G denotes volumetric bedload transport rate; B denotes channel width; u_* denotes shear velocity; \overline{D}_i denotes the mean grain size of the i-th subrange; p_i denotes the volumetric fraction of the i-th subrange in bedload; F_i denotes the volumetric fraction of the i-th subrange in the surface layer; D_{sg} denotes geometric mean grain size of the surface layer; ϕ_{sgo} is normalized Shields stress; ω is a function of the normalized Shields stress ϕ_{sgo} and the arithmetic standard deviation of the surface layer. Coefficients α and β are given as:

$$\alpha = 0.00218; \quad \beta = 0.0951 \quad (\text{Equation A-2a-b})$$

Grain size is described both in diameter and in ψ -scale, which is the negative of the more commonly used ϕ -scale in geophysics community (1990a and 1990b).

$$\psi_i = -\phi_i = \log_2(D_i) \quad (\text{Equation A-3})$$

The grain size is divided into N subgroups bounded by N+1 grain sizes ψ_1 (D_1) to ψ_{N+1} (D_{N+1}). The mean grain size of the i-th subrange is then given as:

$$\overline{\psi}_i = \frac{\psi_i + \psi_{i+1}}{2}, \quad \overline{D}_i = \sqrt{D_i D_{i+1}} \quad (\text{Equation A-4a-b})$$

The surface layer mean grain size $\overline{\psi}_s$ and standard deviation $\sigma_{s\psi}$ are as follows,

$$\overline{\psi}_s = \sum_{i=1}^N \overline{\psi}_i F_i, \quad \sigma_{s\psi}^2 = \sum (\overline{\psi}_i - \overline{\psi}_s)^2 F_i \quad (\text{Equation A-5a-b})$$

and the geometric mean grain size is given as:

$$D_{sg} = 2^{\overline{\psi}_s} \quad (\text{Equation A-5c})$$

Note that the surface based bedload equation of Parker applies only to particles too coarse to be transported in suspension, and Parker further suggested that the finest grain size (D_1) be set as 2 mm as a common rule in field cases (Parker 1990a and 1990b).

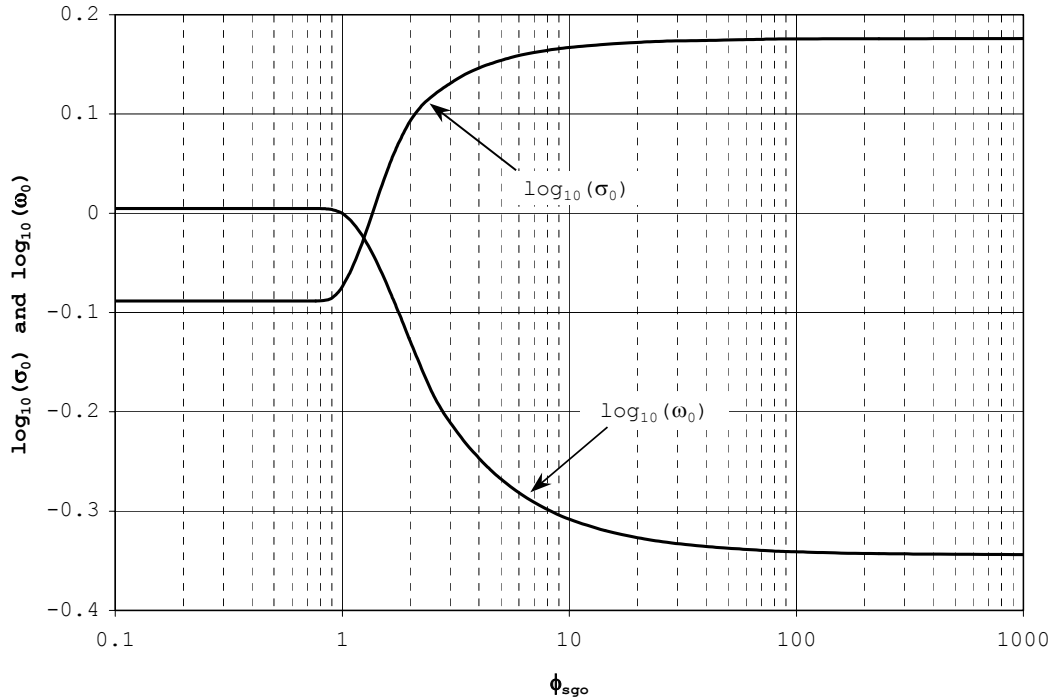


Figure A-1. Parameters σ_0 and ω_0 as functions of ϕ_{sgo} in Parker equation.

Parameter ω is a function of the normalized Shield stress ϕ_{sgo} ,

$$\omega = 1 + \frac{\sigma_0}{\sigma_{sv}} (\omega_0 - 1) \quad \text{(Equation A-6)}$$

where σ_0 and ω_0 are functions of ϕ_{sgo} given in Figure 1 (Parker 1990a and 1990b). The relations can also be found in tabulated form in Parker (1990a and 1990b).

The normalized Shield stress ϕ_{sgo} is acquired by dividing the surface based Shield stress τ_{sg}^* by a reference stress τ_r^* ,

$$\phi_{sgo} = \frac{\tau_{sg}^*}{\tau_r^*} \quad \text{(Equation A-7)}$$

where the reference Shield stress τ_r^* was originally proposed by Parker (1990a and 1990b) as 0.0386.

However, for this study the reference Shield stress τ_r^* was determined from the relation proposed by Mueller et al. (2005) described in detail below (Section 2), which was calibrated with data from the tracer rock study where possible. The surface based Shield stress τ_{sg}^* is defined as:

$$\tau_{sg}^* = \frac{u_*^2}{RgD_{sg}} \quad \text{(Equation A-8)}$$

Shear velocity u_* is assumed to obey the Keulegan resistance relation,

$$\frac{u}{u_*} = 2.5 \ln \left(11 \frac{h}{k_s} \right) \quad \text{(Equation A-9)}$$

in which u denotes flow velocity; h denotes water depth and k_s denotes roughness height. Roughness height is defined slightly differently from the original work of Parker (1990a and 1990b) for simplicity,

$$k_s = 2D_{sg} \sigma_{sg}^{1.28} \quad \text{(Equation A-10)}$$

where σ_{sg} denotes surface layer geometric standard deviation,

$$\sigma_{sg} = 2^{\sigma_{sv}} \quad \text{(Equation A-11)}$$

Note that the roughness height given in Equation (A-10) is an approximation of the original value given by Parker (1990a and 1990b), in which the roughness height was defined as twice of surface layer D_{90} .

In case of a normal flow, shear velocity u_* can be expressed as:

$$u_* = \sqrt{ghS} \quad \text{(Equation A-12)}$$

in which S is channel bed slope.

Function G is given by Parker (1990a and 1990b) as:

$$G(\phi) = \begin{cases} 5474 \left(1 - \frac{0.853}{\phi} \right)^{4.5} & \phi > 1.59 \\ \exp[14.2(\phi - 1) - 9.28(\phi - 1)^2] & 1 \leq \phi \leq 1.59 \\ \phi^{14.2} & \phi < 1 \end{cases} \quad \text{(Equation A-13)}$$

In case of an arbitrary cross section, the cross section is divided into the main channel and a floodplain. In this case sediment transport over floodplain is assumed to be insignificant.

The surface based bedload equation of Parker (Equation A-1) and the Keulegan resistance relation (Equation A-9) are modified as follows,

$$\frac{RQ_G P_i}{A_c S u_*} = \alpha F_i G(\omega \phi_{sgo} (\bar{D}_i / D_{sg})^{-\beta}) \quad \text{(Equation A-14)}$$

$$\frac{u_c}{u_*} = 2.5 \ln \left(11 \frac{R_{hc}}{k_s} \right) \quad \text{(Equation A-15)}$$

where A_c denotes flow area in the main channel; R_{hc} denotes hydraulic radius of the flow in the main channel,

$$R_{hc} = \frac{A_c}{P_c} \quad \text{(Equation A-16)}$$

and P_c denotes the wet perimeter of the main channel. Shear velocity, roughness height and grain size parameters in Equations A-14 and A-15 all refer to those in the main channel.

Floodplain hydraulics and flow continuity are brought in to close the equations,

$$Q_{wf} = \frac{1}{n} A_f R_{hf}^{2/3} S^{1/2} \quad (\text{Equation A-17})$$

$$Q_{wf} + Q_{wc} = Q_w \quad (\text{Equation A-18})$$

$$R_{hf} = \frac{A_f}{P_f} \quad (\text{Equation A-19})$$

$$u_c = \frac{Q_{wc}}{A_c} \quad (\text{Equation A-20})$$

where n denotes Manning's n for floodplain; A_f denotes flow area in floodplain; P_f denotes the wet perimeter of the floodplain; R_{hf} denotes hydraulic radius of the floodplain; Q_{wf} and Q_{wc} denotes the discharge on floodplain and main channel respectively.

The following assumptions and limitations pertain to applying Parker's surface-based bedload equation (Parker 1990a and 1990b in the EASI model):

- Flow is assumed to be normal (steady and uniform) flow.
- Friction slope (energy slope) is approximated by the reach-averaged water surface slope surveyed at relatively low discharges.
- Sediment densities are assumed to be 2,650 kg m⁻³.
- The channel is assumed prismatic (continuous channel shape throughout the reach being modeled) based on the shape of the cross-section input; as a result, cross-sections used in the model should be located in uniform and representative sites of the entire reach.
- If floodplains exist at the cross-section, sediment transport occurs only in the main channel while the floodplains convey part of the flow at discharges that overtop the bank and connect with the floodplain.
- Parker's (1990a and 1990b) bedload transport equation and the EASI model are intended to simulate sediment transport in alluvial reaches. The model is not designed to predict sediment transport capacities in bedrock channels or streams paved with large immobile boulders because large roughness elements can create reach-scale deviations in shear stress that limit the effectiveness of bedload transport equations based on total boundary shear (Yager et al. 2004). However, if an estimated bedload grain size distribution is given under supply-limited conditions, the model can be used to calculate the transport capacity of the bedload supply with a given hydrologic condition. Physical models of steep stream channels with large roughness elements have shown that boulders can reduce sediment transport of mobile grain sizes by absorbing a significant amount of the fluid force, trap sediment that would otherwise be highly mobile, or induce scour and increase sediment transport due to creating turbulent flow structures. Thus, the effect of roughness elements on sediment transport and bed morphology can vary and is difficult to determine, for a given roughness configuration (Yager et al. 2004). Numerical theories and equations developed specifically for predicting bedload transport in boulder dominated systems are currently unavailable, and Parker's (1990a and 1990b) bedload transport equation is deemed the best available option.
- Simulated sediment transport capacities should be viewed as long-term averages.
- As with any sediment transport equation, sediment transport capacities calculated with EASI model can have an error factor of 2 to 3.

DETERMINATION OF REFERENCE SHEAR STRESS AND RANGE OF TRANSPORT ESTIMATES

In order to calculate Q_{cr} and bedload transport capacities a reference Shields stress (τ_r^*) is necessary to evaluate when sediment transport initiates. A reference Shield stress is a Shields stress under which the dimensionless bedload transport rate of different size fractions collapse to a constant low value (commonly referred to as W^*), e.g., 0.00218 in Parker (1990a and 1990b). Reference Shield stresses in this study were determined from tracer rock studies and from published values. In particular, a τ_r^* and channel gradient relationship (Equation A-21) developed by Mueller et al. (2005) based on field measurements of discharge and bedload transport in 45 gravel-bed streams was used for this study:

$$\tau_r^* = 2.18S + 0.021 \quad \text{(Equation A-21)}$$

where S is reach-averaged slope. Mueller et al. (2005) utilized the measured flow and bedload flux measurements collapsed to a W^* of 0.002 to calculate τ_r^* for each reach. Mueller et al. (2005) calculated an R^2 of 0.70 for Equation A-21 and found that the average relative range of τ_r^* for a given slope was 24% from the median value. Equation A-21 was used to estimate τ_r^* for intensive study sites used to model sediment transport for this study.

9 LITERATURE CITED

Mueller, E. R., J. Pitlick, and J. M. Nelson. 2005. Variation in the reference Shields stress for bed load transport in gravel-bed streams and rivers. *Water Resources Research* 41: W04006, doi: 10.1029/2004WR003692

Parker, G. 1990a. Surface-based bedload transport relation for gravel rivers. *Journal of Hydraulic Research* 28: 417-436.

Parker, G. 1990b. The Acronym Series of PASCAL program for computing bedload transport in gravel rivers. External Memorandum M-220. St. Anthony Falls Laboratory, University of Minnesota.

Yager, E., M. Schmeeckle, W. E. Dietrich, and J. W. Kirchner. 2004. The effect of large roughness elements on local flow and bedload transport. American Geophysical Union, AGU Fall Meeting: Abstract #H41G-05.

10 LIST OF NOTATIONS USED IN APPENDIX A

A	area of the flow;
B	channel width;
D_i	the lower bound grain size of the i-th subrange;
$\overline{D_i}$	mean grain size of the i-th subrange ($= \sqrt{D_i D_{i+1}}$);
D_{sg}	geometric mean grain size of the surface layer;
F_i	volumetric fraction of the i-th subrange in the surface layer;
g	acceleration of gravity;
h	water depth;
k_s	roughness height;
P	wet perimeter of the channel;
p_i	volumetric fraction of the i-th subrange in bedload;
Q_G	gravel transport rate;
Q_w	water discharge;
R	submerged specific gravity of gravel;
R_h	hydraulic radius of the flow;
S	reach average channel bed slope;
u	flow velocity;
u^*	shear velocity;
α	coefficient in Parker equation ($= 0.00218$);
β	hiding coefficient in Parker equation ($= 0.0951$);
ϕ_{sgo}	normalized Shield stress;
σ_0	parameter in Parker equation (is a function of ϕ_{sgo});
σ_{sg}	geometric standard deviation of the surface layer;
$\sigma_{s\psi}$	arithmetic standard deviation of the surface layer;
τ_r^*	reference Shield stress;
τ_{sg}^*	Shield stress;
ω	parameter in Parker equation (is a function of $\sigma_{s\psi}$ and ϕ_{sgo});
ω_0	parameter in Parker equation (is a function of ϕ_{sgo});
ψ_i	the lower bound of the i-th subrange grain size in ψ -scale, $\psi_i = \log_2(D_i)$, where D_i is grain size in mm;
$\overline{\psi_i}$	mean grain size of the i-th subrange in ψ -scale ($= \frac{\psi_i + \psi_{i+1}}{2}$);
$\overline{\psi_s}$	mean grain size of the surface layer in ψ -scale.

Appendix E

WDFW escapement and redd count tables

Table E-1. Lewis River fall Chinook escapement estimates, 1984-2005.

Return year(s)	Age class ²					CWT wild ³	Hatchery strays ⁴	Total escapement
	2+	3+	4+	5+	6+ and 7+			
1964–1973 ^{1,5}	3,103	2,060	6,803	2,130		NA	NA	14,096
1974–1983 ^{1,5}	1,155	2,026	6,332	1,911	2	NA	NA	11,425
1984 ⁵	947	1,192	3,582	2,263	95	7,794	285	8,079
1985 ⁵	1,984	1,891	4,046	1,538	16	8,323	1,152	9,475
1986 ⁵	2,578	4,091	5,714	2,112	66	12,878	1,683	14,561
1987 ⁵	4,145	3,469	6,922	2,527	17	16,345	735	17,080
1988 ⁵	2,594	1,786	6,642	3,631		13,766	887	14,653
1989 ⁵	1,788	2,568	6,261	12,210	160	21,832	1,155	22,987
1990 ⁵	1,440	947	7,275	7,692	1,592	16,814	2,132	18,946
1991 ⁵	568	1,252	3,004	4,419	385	9,350	278	9,628
1992 ⁵	1,651	441	3,416	2,128	322	7,153	805	7,958
1993 ⁵	632	2,146	1,216	3,353	310	7,061	596	7,657
1994 ⁵	1,537	1,359	6,926	1,295	356	10,391	1,082	11,473
1995 ⁵	859	1,001	2,915	7,474	25	12,274	0	12,274
1996 ⁵	263	1,277	7,889	4,182	602	12,934	1,279	14,213
1997 ⁵	62	218	4,280	4,125	47	8,227	505	8,732
1998 ⁵	251	940	1,437	4,012	5	5,123	1,522	6,645
1999 ⁵	183	1,118	1,337	942	46	2,595	1,031	3,626
2000 ⁶	1,260	1,393	3,622	549	2	3,068	560	6,826
2001 ⁶	1,124	1,878	5,616	1,537	13	6,419	1,459	10,168
2002 ⁶	1,198	1,895	8,483	4,634	34	10,265	2,371	16,244
2003 ⁷	1,064	1,009	8,247	8,084	175	11,751	3,031	18,579
2004 ⁷	523	2,087	3,881	7,063	428	11,469	757	13,982
2005 ⁷	365	1,235	7,132	2,731	249	9,872	1,021	11,712
10-year average	629	1,305	5,192	3,786	160	8,172	1,354	11,073
20-year average	1,204	1,606	5,111	4,235	254	10,479	1,144	12,397

¹ Average for range of return years.

² Based on scale pattern analysis.

³ Through 1999, Lewis River CWT wild escapement was estimated by subtracting hatchery stray fall Chinook from the total escapement, based on stray CWTs recovered. Beginning in 2000, the CWT wild were estimated from the expansion of the wild CWTs recovered using an expansion rate generated by dividing the total CWTs recovered, after the first Wednesday in November and before the third week in December, by the number of age specific carcasses examined for CWTs (mark rate). The remaining spawners were consider wild Tules (October) and wild Late Brights (December–January).

⁴ Strays were estimated from the recovery of out-of-basin hatchery CWTs.

⁵ Estimate generated from expansion of the peak count by 5.27, which was established from the 1976 carcass tagging project.

⁶ Estimate calculated from sequential analysis of results from the mark recapture of carcasses on the Lewis River, and does not include Cedar Creek escapement.

⁷ Estimates were generated by expanding the age-specific Lewis River mark sample totals by the age-specific average sample rates generated by combining the results from the 2001 and 2002 mark recapture study. Estimates do not include Cedar Creek fall Chinook escapement.

Table E-2. Lewis River CWT wild escapement estimates, 1984-2005.

Return year	Age class						Hatchery strays ²	Total escapement
	2+	3+	4+	5+	6+ and 7+	Total CWT Wild ¹		
1984 ³	947	1,186	3,425	2,141	95	7,794	285	8,079
1985 ³	1,984	1,869	3,280	1,174	16	8,323	1,152	9,475
1986 ³	2,578	3,552	5,293	1,389	66	12,878	1,683	14,561
1987 ³	4,145	3,400	6,266	2,520	17	16,348	732	17,080
1988 ³	2,594	1,734	5,872	3,566	0	13,766	887	14,653
1989 ³	1,774	2,283	6,070	11,545	160	21,832	1,155	22,987
1990 ³	1,436	517	5,803	7,534	1,592	16,882	2,064	18,946
1991 ³	568	1,252	2,720	4,419	385	9,344	284	9,628
1992 ³	1,651	441	2,846	1,893	322	7,153	805	7,958
1993 ³	632	1,999	767	3,353	310	7,061	596	7,657
1994 ³	1,537	1,345	6,399	339	356	9,976	1,497	11,473
1995 ³	859	1,001	2,915	7,474	25	12,274	0	12,274
1996 ³	263	1,050	6,859	4,168	602	12,942	1,271	14,213
1997 ³	59	218	3,778	4,125	47	8,227	505	8,732
1998 ³	234	0	979	3,905	5	5,123	1,522	6,645
1999 ³	180	920	507	942	46	2,595	1,031	3,626
2000 ⁴	793	649	1,626	0	0	3,068	560	6,826
2001 ⁴	787	1,006	3,638	987	0	6,418	1,459	10,168
2002 ⁴	918	1,110	5,123	3,114	0	10,265	2,371	16,244
2003 ⁴	902	481	4,376	5,870	121	11,750	3,031	18,579
2004 ⁴	502	1,619	2,830	6,174	345	11,470	757	13,982
2005 ⁴	356	1,012	6,313	1,980	211	9,872	1,021	11,712
10-year average	499	807	3,603	3,127	138	8,173	1,353	11,073
20-year average	1,138	1,279	4,049	3,765	243	10,462	1,162	12,397

¹ Through 1999, Lewis River CWT wild escapement was estimated by subtracting hatchery stray fall Chinook from the total escapement, based on stray CWTs recovered. Beginning in 2000, the CWT wild were estimated from the expansion of the wild CWTs recovered using an expansion rate generated by dividing the total CWTs recovered, after the first Wednesday in November and before the third week in December, by the number of age specific carcasses examined for CWTs (mark rate). The remaining spawners were consider wild Tules (October) and wild Late Brights (December–January).

² Strays were estimated from the recovery of out-of-basin hatchery CWTs.

³ Estimate generated from expansion of the peak count by 5.27, which was established from the 1976 carcass tagging project.

⁴ Estimate calculated from sequential analysis of results from the mark recapture of carcasses on the Lewis River, and does not include Cedar Creek escapement.

⁵ Estimates were generated by expanding the age-specific Lewis River mark sample totals by the age-specific average sample rates generated by combining the results from the 2001 and 2002 mark recapture study. Estimates do not include Cedar Creek fall Chinook escapement.

Table E-3. Peak fall Chinook redd counts in the North Fork Lewis River.

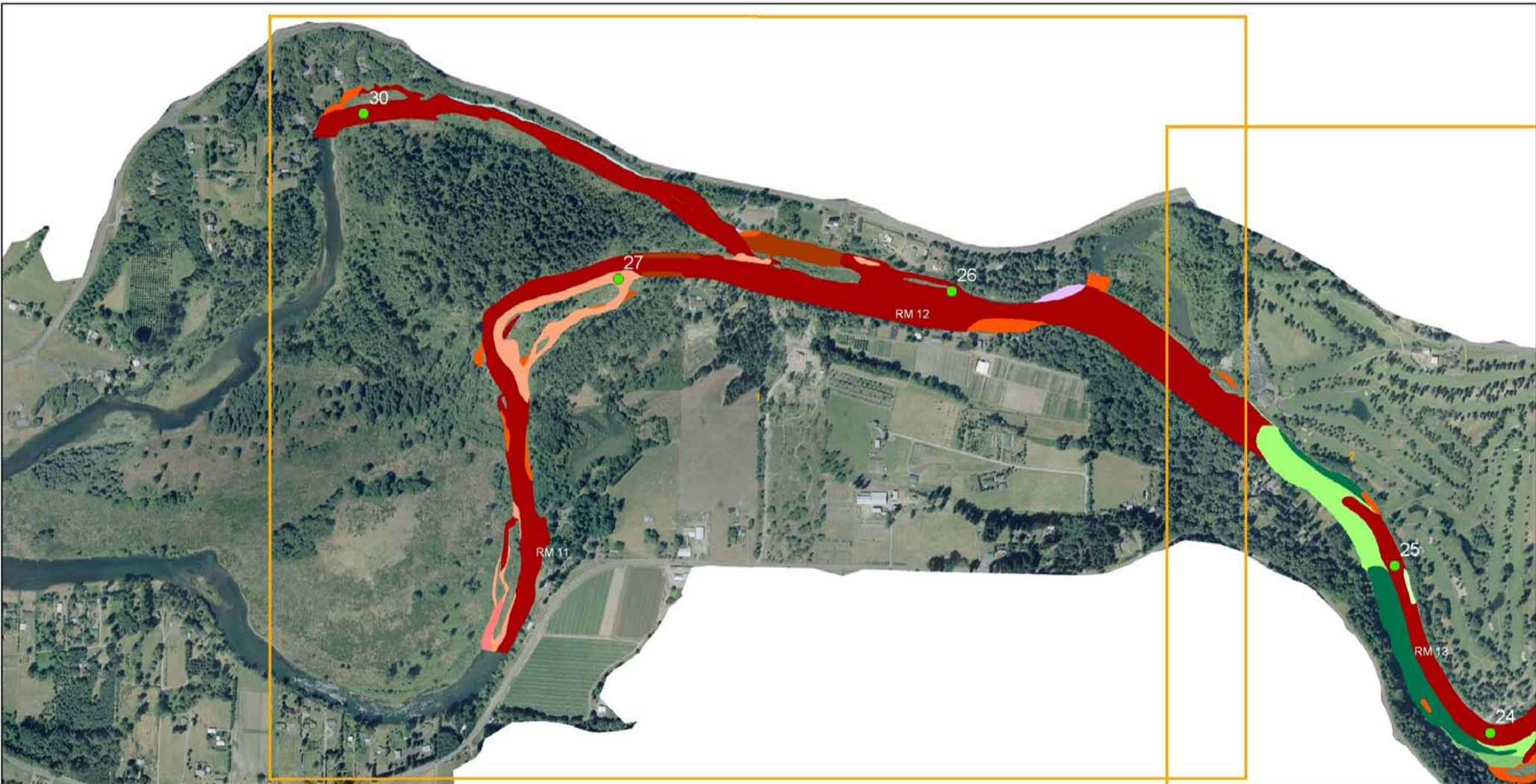
Year	Date	Index reach ¹			
		1	2	3	4
1971	14-Nov	577	639	727	210
1972	12-Nov	400	774	703	237
1973	11-Nov	332	377	431	133
1974	9-Nov	229	91	249	98
1975	13-Nov	699	545	637	178
1976	12-Nov	163	167	147	38
1977	20-Nov	335	375	174	61
1978	30-Nov	207	146	123	59
1979	15-Nov	281	223	87	19
1980	17-Oct	249	131	137	142
1981	5-Nov	158	203	169	89
1982	24-Nov	382	298	233	41
1983	1-Dec	297	263	207	74
1984	15-Nov	473	330	213	91
1985	14-Nov	274	215	127	59
1986	20-Nov	252	225	169	79
1987	19-Nov	309	254	177	99
1988	3-Nov	156	182	248	178
1989	16-Nov	334	171	304	148
1990	15-Nov	498	394	360	183
1991	21-Nov	412	190	135	25
1992	19-Nov	335	201	152	58
1993	18-Nov	178	144	119	58
1994	17-Nov	280	189	217	75
1995	9-Nov	493	283	298	119
1996	14-Nov	288	620	393	205
1997	20-Nov	237	295	376	104
1998	19-Nov	231	297	192	100
1999	18-Nov	104	104	85	0

¹ Index Reach 1 is from the Lewis River Hatchery (RM 15.7) upstream to RM 16.7, index reach 2 is from RM 16.7 upstream to RM 17.8, index reach 3 is from RM 17.8 upstream to RM 18.5, and index reach 4 is from RM 18.5 upstream to Merwin Dam (RM 19.5).

Appendix F
Facies mapping

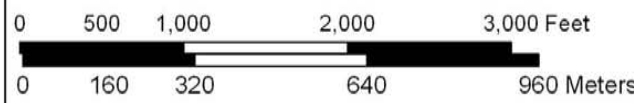
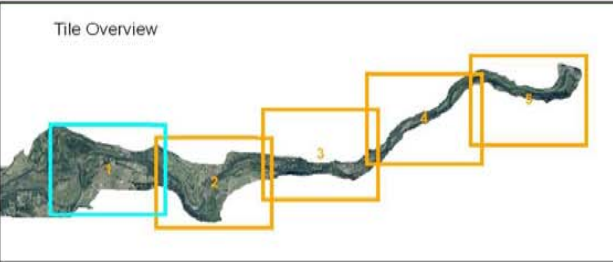
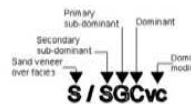
Facies maps (Figures Fa–e) show that the cG_{vc} and gC_f facies are the predominant facies in the evaluation area. Initial field observations, later confirmed by the pebble count data show that in many cases the percent mixture of cobble and gravel on the stream bed is approximately 50% cobble and 50% gravel. However, a distinct pattern of facies types is present above and below the confluence with Cedar Creek (RM 15.7). The reach of the Lewis River above this confluence RM 15.7 (the upper reach) is dominated by gC_f , which has a mean D_{50} of 63.1 mm, whereas the reach below RM 15.7 (the lower reach) is cG_{vc} , which has a mean D_{50} of 46.7 mm. A statistical comparison confirms that the D_{50} for each reach is distinct, likely reflecting the input of finer particles from this significant tributary. The mean sorting coefficient (sc), a measure of dispersion of particle size the pebble counts, is also distinct for each reach. The upper reach has a more poorly sorted bed (sc of 32) than the lower reach (sc of 24). The mean D_{84} for each reach is also different; the upper reach has mean D_{84} of 99.4 mm compared the lower reach with a mean D_{84} of 75.5 mm. The higher D_{84} for the upper reach shows that overall the upper reach has a distinctly coarser surface layer than the lower reach. Thus, while overall the bed of the river in the evaluation area is similar; there are two distinct regimes of facies types in the river. Pebble count data used for Evaluation Area analyses is given in Table F-1.

In addition to the sediment input from Cedar Creek, the physiographic setting of the river valley abruptly shifts at about RM 14.8 from a channel confined by bedrock terraces to a relatively unconfined channel bounded by alluvial fill terraces. The shift in to an overall finer facies is consistent with this physiographic shift, as is the overall widening of the channel and the emergence of large mid-channel bars and islands. It is probable that channel slope is different between the upper and lower reaches, which would also have an effect on transport capacity and thus facies types. Slope surveys in 2006 will delineate the actual channel slope in the two reaches more precisely than can be inferred from existing topographic data.



Lewis River Tile 1 - Facies map

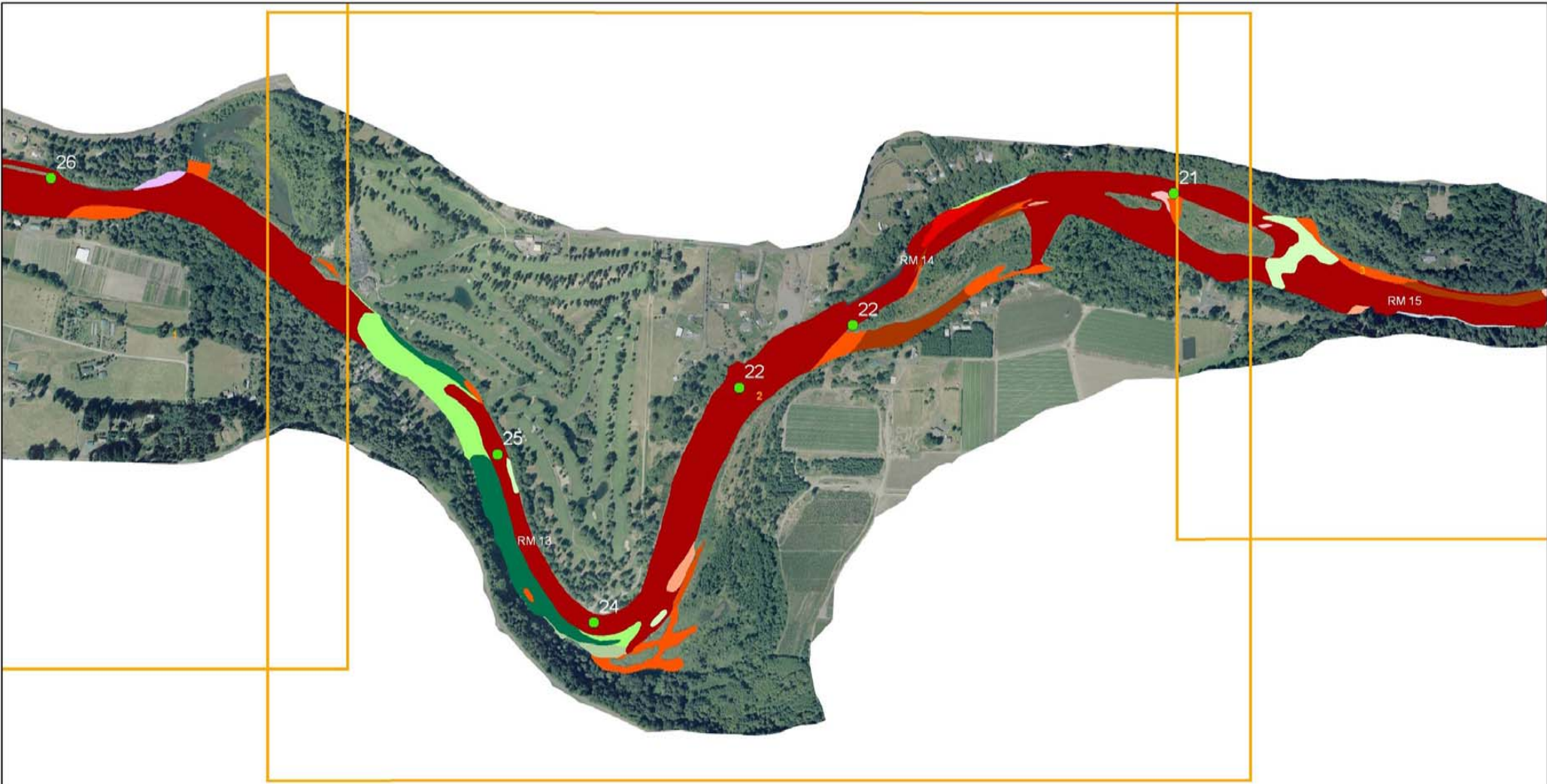
Gravel Facies		Cobble Facies		Boulder Facies		Bedrock Facies	
Gm	SGvc	Gcf	BGcf	Bf	BR		
Ge	CGf	SGCo	BCf	CBf			
Gvc	CGe	BCve	BCe	GCBf			
SlGvc	CGvc	GCc	GBCvc				
SGvf	SGCvc	pebble counts					
SGm	BCGm	Tracersite Locations					



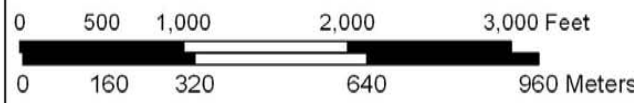
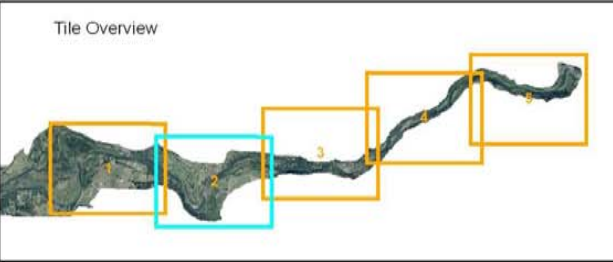
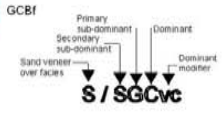
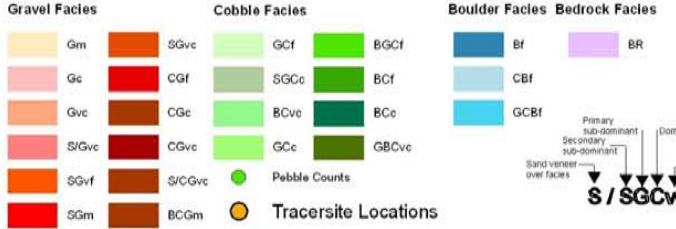
Flow Direction ←



Figure F1. Facies map, Tile 1.



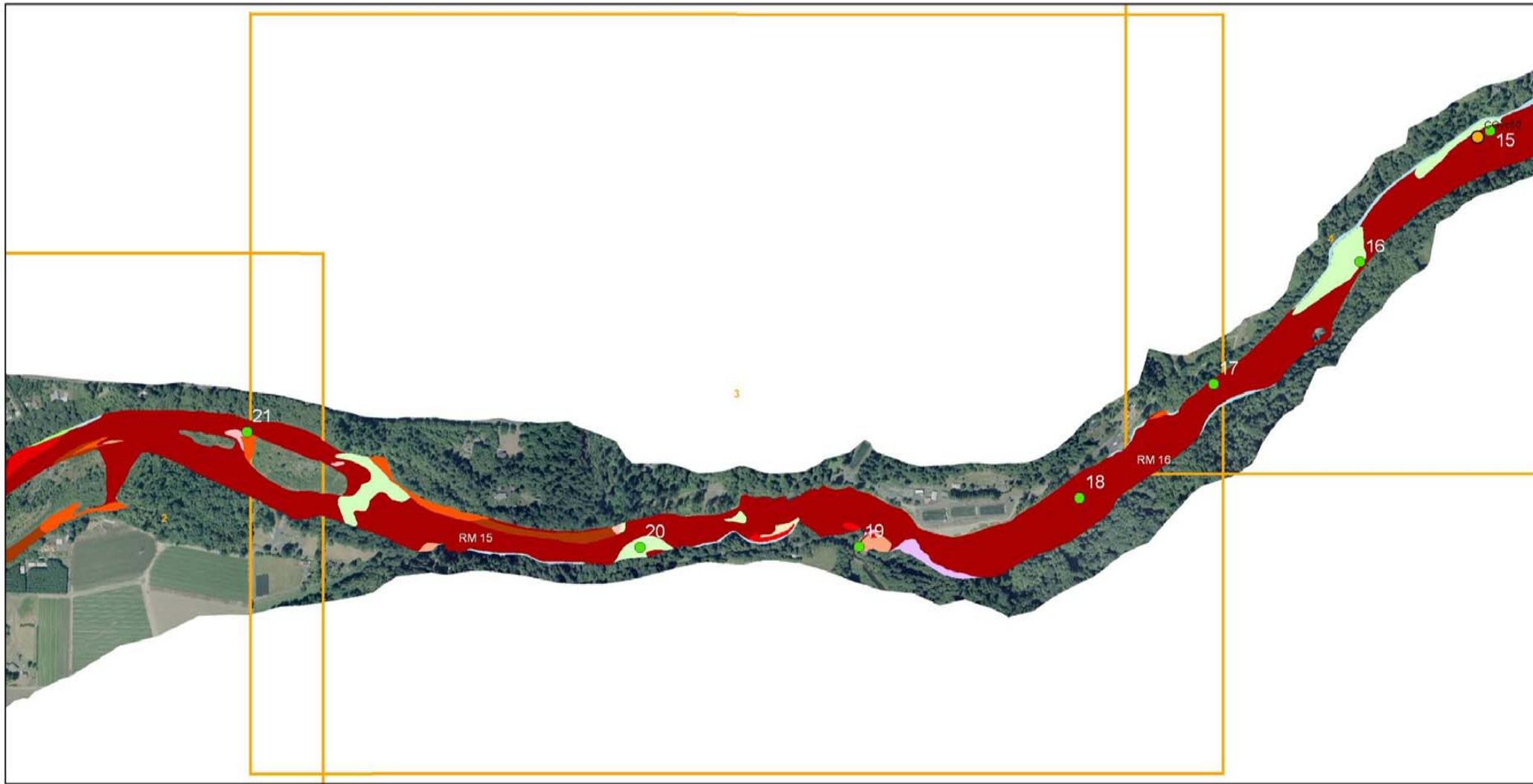
Lewis River Tile 2 - Facies map



← Flow Direction



Figure F2. Facies map, Tile 2.



Lewis River Tile 3 - Facies map

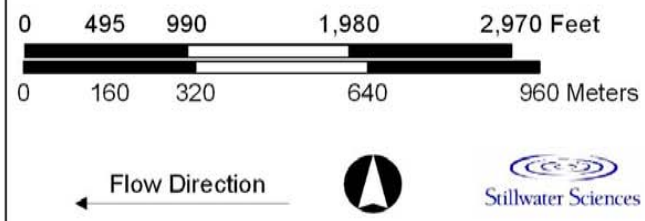
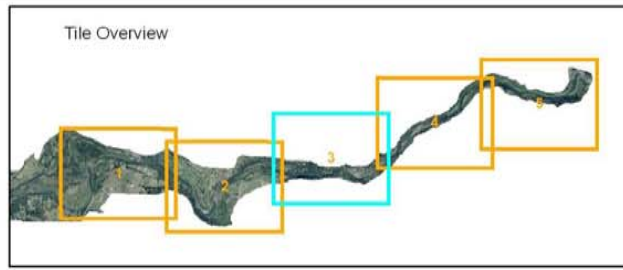
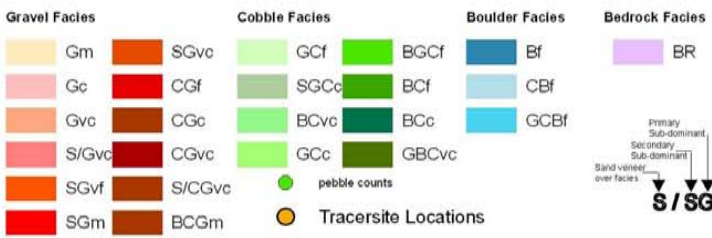
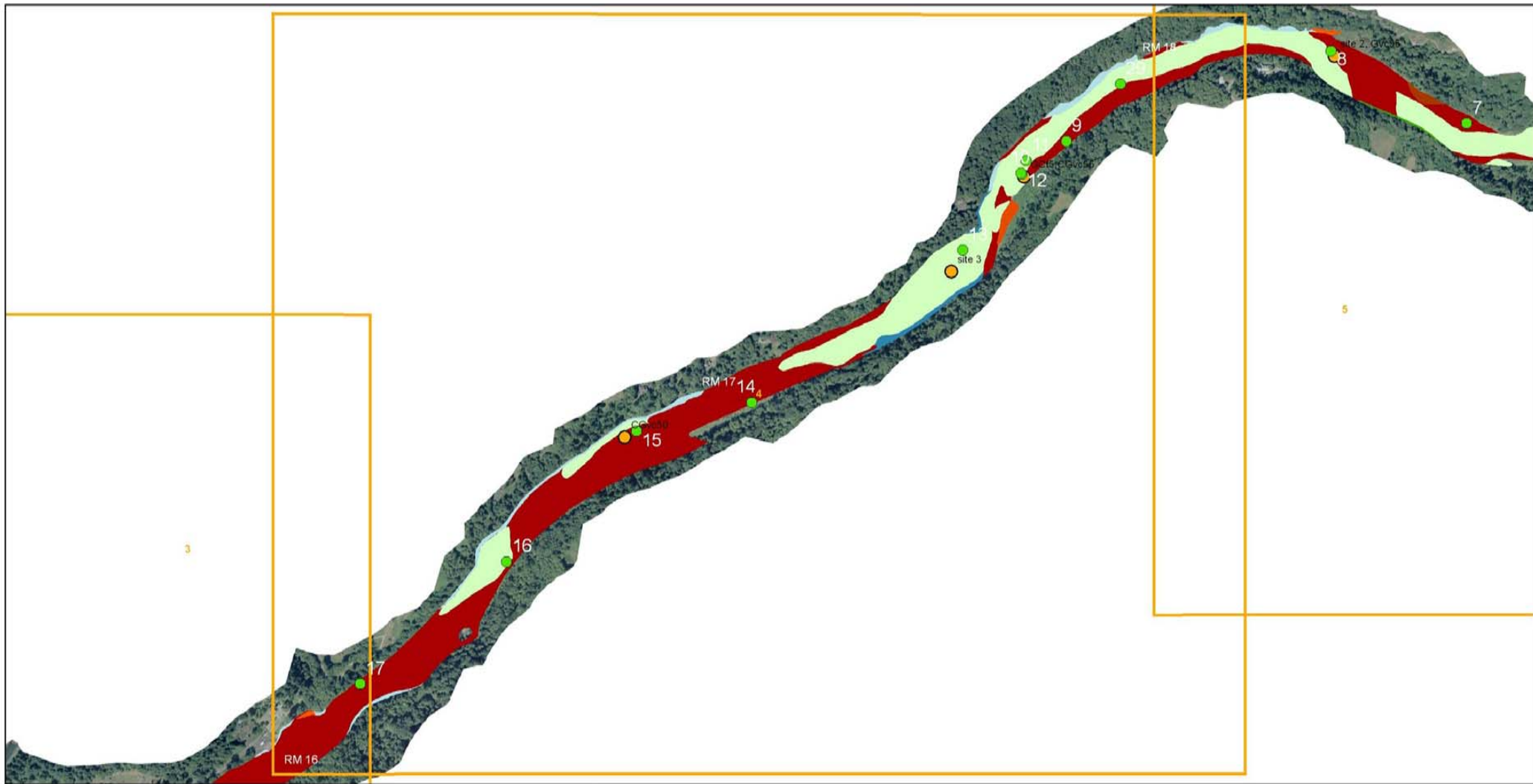


Figure F3. Facies map, Tile 3.



Lewis River Tile 4 - Facies map

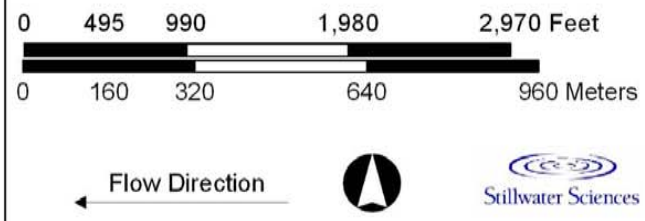
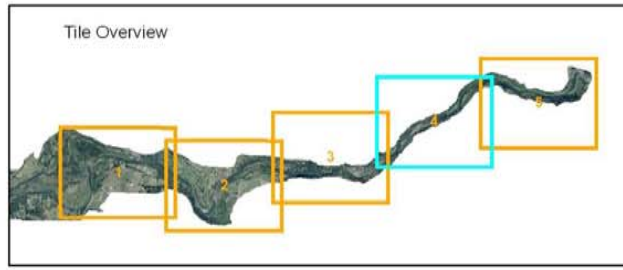
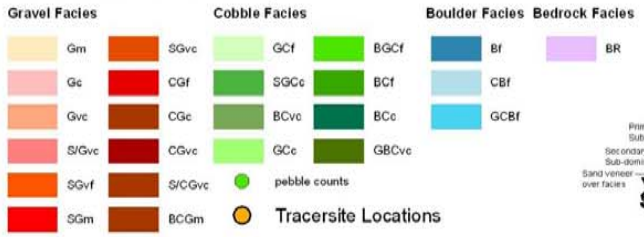
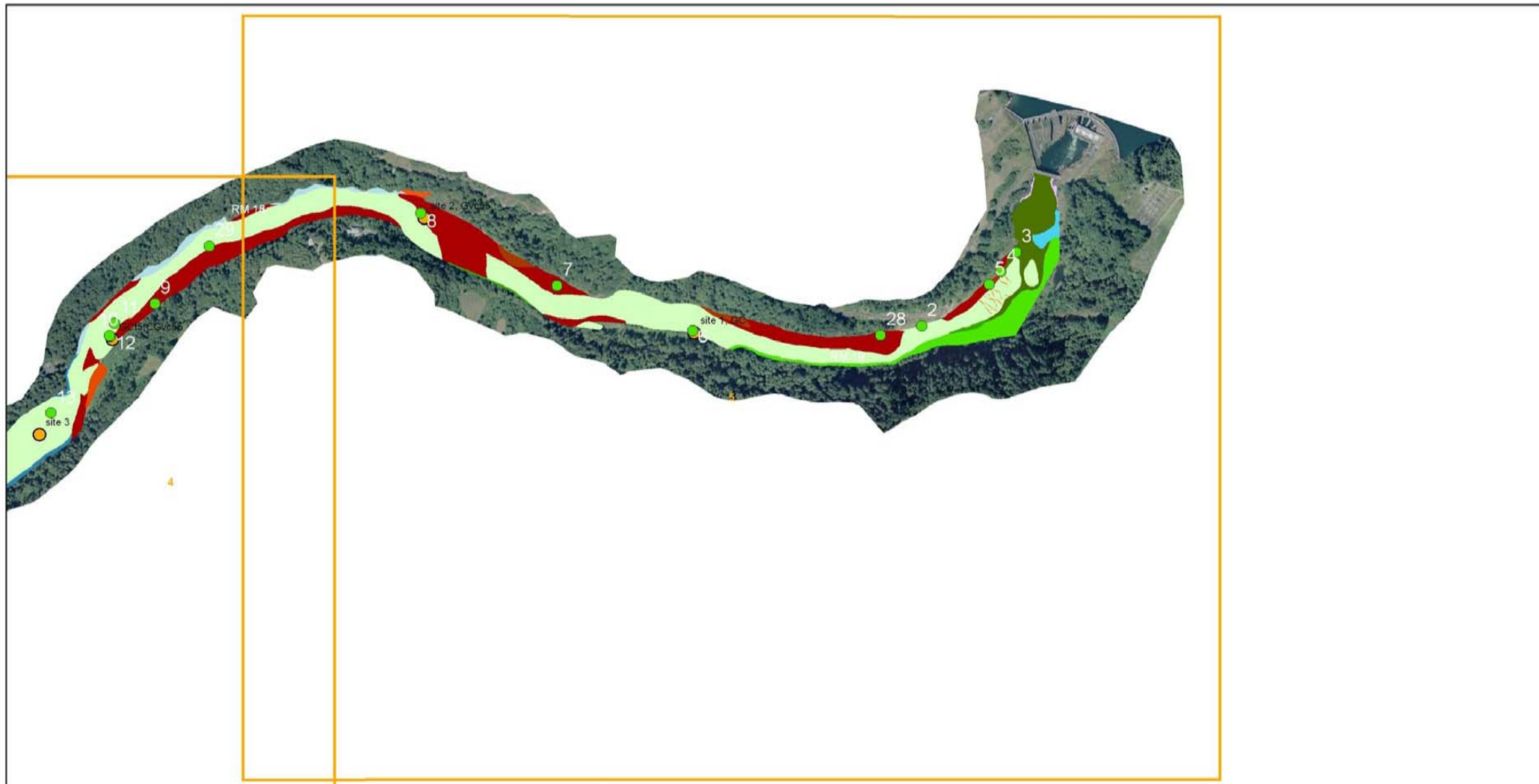
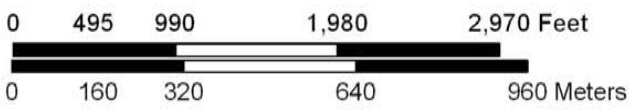
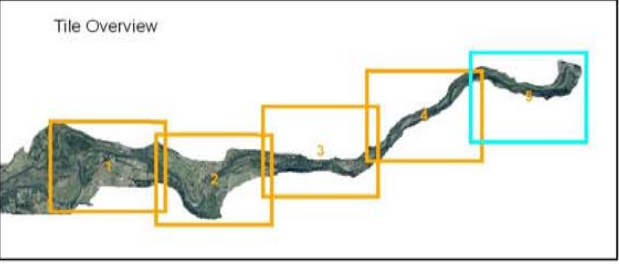
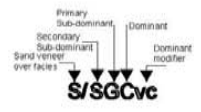
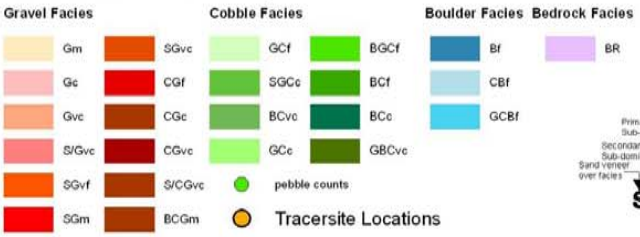


Figure F4. Facies map, Tile 4.



Lewis River Tile 5 - Facies map



Flow Direction ←



Figure F5. Facies map, Tile 5.

Table F-1. Pebble counts in the Evaluation Area for 2005.

Percent finer	Pebble count number																													
	1	2	3	4	5	6	7	8	9	10	11	12	13	14	15	16	17	18	19	20	21	22	23	24	25	26	27	28	29	30
	Particle size (mm)																													
0	5	10	1	1	1	12	1	1	4	4	5	4	29	26	8	1	1	6	1	13	9	1	2	4	15	19	1	1	23	13
1	6	10	1	2	2	20	2	5	9	8	29	7	32	28	13	6	2	10	1	15	12	7	2	13	21	21	2	1	25	16
2	6	17	5	2	3	36	6	6	12	13	34	7	33	30	19	7	2	13	1	15	15	8	6	18	22	22	3	2	36	17
3	6	22	18	2	3	36	6	8	15	15	36	8	34	31	20	9	2	18	2	21	18	9	7	18	23	23	6	4	42	20
4	7	26	21	2	7	37	7	8	18	15	36	8	34	33	21	12	2	20	2	27	22	18	11	20	25	27	6	6	42	20
5	7	26	32	2	8	44	8	10	21	19	46	9	35	33	22	15	6	21	2	27	22	19	12	21	25	27	9	7	45	23
6	8	27	45	2	8	51	10	11	22	24	50	11	35	35	22	16	6	23	2	27	22	20	13	22	26	28	9	10	45	23
7	9	28	53	2	9	57	10	11	22	27	50	18	35	35	23	17	7	23	2	28	22	21	15	25	26	29	10	11	52	23
8	9	31	54	4	9	58	10	12	23	28	53	18	38	36	24	25	9	24	2	31	23	22	16	26	26	29	10	12	53	23
9	9	33	55	4	11	58	11	12	23	31	55	22	40	38	24	25	9	27	2	33	23	23	19	26	28	30	11	13	54	26
10	10	35	56	4	12	59	12	14	26	33	55	26	40	38	26	25	11	27	2	34	24	26	20	27	30	30	11	14	55	28
11	11	35	59	8	13	59	13	15	26	34	56	30	40	39	28	26	13	30	2	35	26	26	22	27	31	30	12	14	57	28
12	12	39	66	8	15	60	14	15	28	36	57	30	42	39	29	26	14	33	2	36	26	27	22	30	32	32	12	15	57	30
13	12	40	66	8	15	60	14	17	28	39	58	34	45	41	30	27	15	33	2	38	26	28	22	31	32	33	12	21	57	31
14	12	42	68	9	15	61	14	18	29	39	60	36	46	42	30	28	15	34	2	40	26	30	22	32	32	33	13	22	58	32
15	12	47	69	9	15	62	15	18	31	40	60	36	46	42	32	29	16	34	4	42	26	30	25	32	32	33	13	22	59	33
16	12	50	71	10	16	64	15	19	32	40	60	36	49	42	34	29	16	37	4	43	27	31	26	32	32	34	13	24	59	33
17	13	51	73	10	17	65	15	19	32	40	60	36	49	43	35	30	17	37	4	46	28	32	26	34	32	34	13	25	61	33
18	13	52	74	10	18	67	16	20	34	41	60	37	50	44	36	31	18	37	4	46	29	33	26	34	33	37	14	26	61	34
19	14	54	76	10	18	68	16	20	35	42	61	37	50	44	36	34	19	38	4	46	29	33	28	36	34	39	14	27	62	35
20	15	55	82	11	18	68	18	21	35	42	63	38	53	44	38	35	20	39	4	46	31	35	30	36	35	39	15	28	62	35
21	16	55	85	11	21	68	18	21	37	45	63	39	55	45	38	35	20	39	4	47	31	35	30	36	36	40	15	28	62	35
22	16	57	87	12	22	72	19	21	38	45	64	39	55	45	39	36	21	41	4	47	32	35	31	36	38	41	16	28	63	35
23	16	63	88	12	23	75	20	22	38	45	64	40	55	46	41	37	23	41	5	47	32	37	33	37	39	42	16	29	63	35
24	18	64	88	13	23	77	20	22	38	45	65	42	55	46	43	38	23	41	5	49	32	38	35	37	40	43	18	31	63	36
25	18	66	89	13	23	77	21	23	39	46	65	45	58	48	44	40	25	48	5	50	32	38	35	38	40	44	20	31	64	37
26	19	67	90	13	24	80	22	23	39	48	65	47	58	48	44	40	25	49	5	50	32	39	35	40	40	44	20	32	64	37
27	19	67	90	14	25	80	22	24	43	49	65	49	60	49	44	40	25	50	6	51	32	39	36	40	40	44	20	32	65	37
28	19	68	91	15	27	80	23	25	45	49	66	50	62	50	44	41	25	50	6	51	33	40	36	42	40	45	20	33	67	38
29	20	68	91	15	28	80	24	25	45	50	66	50	63	50	45	43	26	51	6	51	34	40	41	42	40	45	21	33	70	39
30	20	68	94	15	28	80	24	26	45	50	67	51	63	50	46	43	26	53	6	53	34	40	41	42	41	47	21	34	70	40

Percent finer	Pebble count number																													
	1	2	3	4	5	6	7	8	9	10	11	12	13	14	15	16	17	18	19	20	21	22	23	24	25	26	27	28	29	30
	Particle size (mm)																													
31	20	70	95	15	29	80	25	26	47	50	67	51	63	50	46	45	29	54	6	54	35	40	41	42	41	47	21	34	70	41
32	20	70	96	15	31	81	25	27	47	51	68	51	63	50	47	46	30	55	8	55	36	41	42	42	41	49	22	35	70	41
33	20	70	99	15	31	82	25	28	49	51	68	52	64	51	48	46	30	56	8	55	36	41	43	43	42	49	22	35	72	41
34	21	70	103	15	32	83	26	28	51	51	69	55	64	53	50	47	30	56	8	56	37	42	44	44	42	50	23	37	72	41
35	21	72	104	15	33	84	28	28	52	52	69	57	65	53	50	47	30	57	9	56	38	42	45	44	42	52	24	40	73	44
36	22	72	104	16	33	87	28	29	54	54	70	58	65	54	50	50	32	58	9	56	38	44	45	45	43	52	24	40	73	44
37	22	72	105	16	33	88	30	29	54	54	70	58	65	55	50	52	32	59	9	57	39	47	46	45	44	53	25	41	75	44
38	22	72	106	17	34	88	31	30	55	54	70	60	65	55	50	52	32	59	9	57	39	47	48	45	44	53	25	41	76	45
39	23	72	106	20	35	89	32	30	55	54	71	62	65	56	50	54	34	59	10	57	40	48	48	45	45	54	25	41	77	45
40	23	73	108	20	37	90	32	30	56	55	73	62	66	56	52	56	34	60	11	58	40	49	48	46	45	54	25	44	77	47
41	24	75	108	20	37	90	32	31	56	55	74	63	66	56	52	56	35	60	12	59	41	50	50	46	45	54	26	44	77	47
42	24	75	110	21	38	90	35	32	56	55	74	64	66	57	55	57	35	61	13	60	42	50	50	49	45	54	26	45	78	47
43	24	75	110	21	38	90	38	32	56	55	76	64	68	58	55	58	36	61	13	60	43	52	50	49	46	55	29	46	79	47
44	24	75	110	22	38	93	39	32	57	55	76	65	70	58	55	58	37	62	14	60	43	52	51	49	46	55	29	46	79	48
45	26	75	111	22	39	93	39	34	57	55	77	65	70	58	55	58	38	62	14	61	44	54	52	50	46	56	30	47	79	49
46	26	76	112	22	40	95	40	34	58	56	78	66	70	58	55	59	38	62	14	61	44	55	52	50	46	56	32	49	80	49
47	26	76	115	22	41	97	40	34	58	57	78	66	70	58	58	60	40	62	16	65	45	55	53	50	47	59	32	50	81	49
48	27	78	121	26	42	97	40	34	58	58	78	66	71	59	60	62	40	67	16	65	45	55	53	51	47	60	32	50	81	49
49	28	80	124	26	46	98	40	35	58	59	80	66	72	60	60	63	40	67	16	66	45	55	53	51	48	60	33	51	82	50
50	28	80	126	28	50	98	41	35	58	60	82	67	72	60	60	65	40	68	16	66	46	55	54	52	48	61	33	52	83	51
51	29	82	129	28	52	100	42	35	59	60	83	70	73	62	61	65	40	69	18	66	47	56	55	53	48	65	33	52	83	52
52	30	82	130	30	53	100	44	36	59	61	84	70	75	62	62	67	40	69	18	66	49	56	55	54	49	65	33	52	83	52
53	30	84	131	30	54	102	45	36	59	62	85	72	75	63	64	67	40	70	20	68	49	56	56	54	50	66	33	53	83	53
54	31	84	132	30	56	102	45	36	60	63	87	73	76	63	65	69	40	70	20	70	50	57	56	55	50	68	33	53	85	54
55	31	84	133	32	56	103	45	37	60	64	87	74	76	63	65	70	41	71	20	70	50	58	56	55	51	70	33	55	87	56
56	32	87	135	35	58	103	45	38	60	65	88	74	78	64	66	70	42	73	20	71	51	58	56	55	51	71	35	56	88	57
57	33	88	135	36	58	104	46	39	60	66	88	74	78	65	66	73	42	73	21	71	52	59	58	55	51	72	35	56	88	57
58	35	89	135	38	59	104	47	40	60	66	88	75	80	66	69	75	45	73	21	72	54	59	58	56	52	72	35	58	88	58
59	35	89	137	38	60	104	47	40	61	68	89	76	82	68	70	75	45	74	21	74	54	60	59	56	52	73	36	59	88	58
60	39	90	137	40	60	105	47	42	62	69	89	77	82	68	70	76	45	76	22	75	55	60	60	56	52	74	36	61	88	59
61	40	90	138	40	60	105	47	42	62	70	90	77	83	68	70	76	45	79	23	75	55	62	60	57	52	76	36	62	88	59
62	42	90	140	42	64	105	48	43	62	70	90	81	84	70	70	77	46	80	23	75	55	64	63	58	52	76	38	65	89	60

Percent finer	Pebble count number																													
	1	2	3	4	5	6	7	8	9	10	11	12	13	14	15	16	17	18	19	20	21	22	23	24	25	26	27	28	29	30
	Particle size (mm)																													
63	42	90	142	42	64	106	48	44	63	72	90	81	85	70	72	79	50	82	23	76	56	65	63	58	53	77	38	66	89	61
64	43	92	142	42	65	107	49	45	66	73	90	81	85	71	74	81	50	83	25	77	56	66	65	59	53	78	39	66	89	62
65	46	93	143	43	65	108	50	45	67	75	91	82	85	71	76	85	52	83	28	78	59	66	66	60	53	78	39	66	90	62
66	46	95	145	45	66	109	50	45	67	76	91	84	86	73	77	86	52	84	28	78	59	67	68	61	53	78	41	67	90	62
67	48	96	145	50	66	110	50	45	67	78	92	85	86	73	80	86	52	84	31	78	60	69	69	62	53	79	41	68	90	62
68	48	96	145	52	70	110	52	46	70	79	93	86	88	74	80	90	53	86	32	78	60	69	70	62	54	80	42	70	91	63
69	48	98	150	66	71	110	52	47	70	80	94	86	90	76	81	90	53	88	32	78	61	70	70	63	55	80	42	70	91	63
70	50	98	155	70	74	112	53	48	72	80	95	87	90	77	83	90	53	88	32	80	62	70	72	65	55	82	42	70	91	66
71	50	99	157	72	77	115	54	48	72	82	97	88	90	78	86	91	54	89	32	81	63	70	73	65	55	83	42	70	92	67
72	50	100	157	72	77	115	55	48	76	82	98	90	90	78	87	92	56	89	34	81	63	70	75	65	57	85	44	71	93	67
73	55	102	164	75	77	115	56	50	77	84	98	90	90	80	88	92	58	90	35	82	64	72	75	66	57	85	46	73	93	67
74	57	103	165	75	78	115	57	50	77	84	98	91	95	80	90	92	58	92	35	82	64	75	76	66	58	86	46	74	93	67
75	58	104	168	80	80	115	58	50	78	84	100	92	100	82	90	94	58	92	36	83	65	76	78	66	58	87	47	74	94	67
76	60	105	172	80	80	117	60	51	80	84	100	92	100	82	90	95	59	95	40	85	65	78	80	67	60	87	47	74	94	68
77	60	105	175	82	81	120	61	52	81	85	101	93	102	83	90	96	59	95	40	85	66	79	80	67	60	89	47	75	95	69
78	61	110	185	90	82	120	62	53	81	89	102	93	102	83	92	96	60	99	40	87	70	80	81	69	61	89	47	76	97	70
79	62	110	192	90	82	120	63	53	82	90	103	93	105	84	95	97	62	101	42	89	70	80	82	71	62	92	48	77	98	70
80	65	110	192	92	83	122	64	54	83	91	104	94	105	85	95	97	62	102	42	90	70	81	83	72	62	94	50	78	98	72
81	65	112	193	96	83	124	65	54	84	92	108	94	105	85	99	98	63	102	43	90	70	82	83	72	63	95	51	78	99	72
82	65	112	193	100	83	125	67	54	84	93	109	95	105	86	100	98	65	102	43	91	70	82	85	74	64	95	52	81	100	72
83	66	113	195	102	85	125	70	54	85	95	110	95	110	86	100	100	65	102	45	94	72	83	86	75	65	96	52	81	100	72
84	69	113	200	125	86	128	71	55	86	95	110	96	112	88	102	100	65	102	45	95	72	83	90	76	66	98	53	84	101	73
85	70	114	205	128	88	130	75	60	86	95	110	96	112	89	102	102	65	105	46	97	73	83	93	77	66	98	56	85	102	74
86	71	115	210	135	94	133	77	62	87	96	114	97	115	90	105	104	65	106	52	99	73	85	93	81	68	100	56	86	103	75
87	72	115	230	151	96	135	80	62	88	96	115	98	119	90	108	106	66	112	52	100	73	86	95	82	69	100	61	90	107	76
88	75	115	232	155	96	140	80	63	89	103	115	101	120	91	108	107	66	113	53	101	78	86	96	85	69	103	64	91	107	76
89	76	117	250	162	98	140	84	63	89	104	115	103	120	93	109	108	72	115	53	105	79	90	99	88	71	104	64	92	108	79
90	77	120	260	228	100	150	84	70	90	105	117	105	121	94	110	109	72	118	58	106	80	94	100	89	72	104	64	95	114	80
91	78	122	265	240	102	150	84	70	91	110	118	107	121	98	118	110	72	120	58	110	82	96	103	90	72	105	66	96	115	80
92	78	123	275	240	106	152	85	70	92	113	123	108	125	101	120	111	77	121	58	111	82	96	109	92	72	106	66	96	119	81
93	79	125	280	260	110	157	85	73	98	115	124	109	128	102	121	117	82	121	60	112	85	98	110	92	73	108	67	100	120	84
94	80	130	280	260	113	165	88	76	110	117	127	111	132	107	125	118	82	123	62	116	85	100	111	96	75	110	67	104	121	86

Percent finer	Pebble count number																													
	1	2	3	4	5	6	7	8	9	10	11	12	13	14	15	16	17	18	19	20	21	22	23	24	25	26	27	28	29	30
	Particle size (mm)																													
95	80	135	290	280	128	170	94	76	112	120	127	112	134	108	125	123	82	125	63	117	86	103	115	100	76	111	70	106	121	87
96	80	177	300	295	133	178	100	77	112	123	132	112	141	110	140	125	82	125	64	120	89	105	122	102	79	112	70	111	123	92
97	82	205	330	330	134	179	110	87	113	125	138	116	146	112	150	130	86	126	74	125	89	112	140	102	80	125	70	113	125	95
98	82	215	335	370	150	188	118	91	116	131	145	120	150	125	158	135	100	130	120	132	90	115	142	104	81	138	72	119	131	96
99	91	260	440	380	165	195	120	109	120	143	190	120	170	170	160	136	104	137	126	139	103	122	145	122	92	138	82	131	135	102